A

DISSERTATION REPORT

on

RESPONSE OF CONTAINMENT STRUCTURE WITH NONLINEAR SOIL-STRUCTURE INTERACTION

Submitted in partial fulfilment of the

requirements for the award of the degree

of

MASTER OF TECHNOLOGY

in

EARTHQUAKE ENGINEERING

(With Specialization in Structural Dynamics)

Submitted by

RAMA DABADGE

DEPARTMENT OF EARTHQUAKE ENGINEERING
INDIAN INSTITUTE OF TECHNOLOGY, ROORKEE

ROORKEE-247667, INDIA
MAY, 2016

CANDIDATES DECLARATION

I, Rama Dabadge hereby declare that the work which is being presented in this seminar report entitles, **"RESPONSE OF CONTAINMENT STRUCTURE WITH NONLINEAR SOIL- STRUCTURE INTERACTION**" in partial fulfillment for the award of the degree of **MASTER OF TECHNOLOGY** in **EARTHQUAKE ENGINEERING,** with specialization in **STRCUTURAL DYNAMICS**, submitted in the Department of Earthquake Engineering, Institute of Technology, Roorkee , is an authentic record of my own work carried out for a period from Aug 2015 to April 2016 under the supervision of Dr. D.K. Paul, Emeritus Fellow, Department of Earthquake Engineering , Indian Institute of Technology, Roorkee.

The matter embodied in this report has not been submitted by me for the award of any other degree or diploma of this institute or any other University/Institute.

Place: Roorkee

Date:

Rama Dabadge

M.Tech Structural Dynamics
Department of Earthquake Engineering

I.I.T Roorkee

CERTIFICATE

This is to certify that the above statement made by the candidate is correct to the best of my knowledge.

Place: Roorkee

Date:

Dr.D.K.Paul

Emeritus Fellow
Department of Earthquake Engineering

I.I.T Roorkee

ACKNOWLEDGEMENT

I would like to express my deepest gratitude to Dr.D.K.Paul, Emeritus fellow, Department of Earthquake Engineering, IIT Roorkee, for his careful guidance, timely suggestions and constant encouragement throughout the course of preparing this report.

Place: Roorkee

Rama Dabadge

Date:

M.Tech Structural Dynamics
Department of Earthquake Engineering

I.I.T Roorkee

ABSTRACT

Design of critical facilities such as nuclear power plant requires an accurate evaluation of seismic demands, as any failure of these facilities poses huge threat to the community. Design complexity of these structures enforces the inevitability of a robust 3D modeling and the soil-foundation interface.

This report includes past research related to effect of soil structure interaction especially on nuclear facilities. Analytical model of NPP along with the underlying soil presented here. Finite element model of nuclear structure and soil surrounding to it is done using F.E software Abaqus. For superstructure, concrete damage plasticity model has been adopted. Concrete damage plasticity model has been validated with three point beam problem. Reinforcements in superstructure are modeled as truss elements and embedded in concrete with the assumption of full bond with surrounding concrete. Soil is modeled as an elastoplastic material using Mohr-Coulomb failure criteria. To avoid reflection of waves back into problem domain absorbing boundaries are used at the finite soil boundaries. Dashpot elements are used as absorbing boundaries which eliminates box effect and act as quite boundaries. Mesh convergence tests have been performed before adopting mesh of the structure and soil for analysis. Change in fundamental time period of structure after introduction of soil has been observed. Also, response of nuclear containment structure in terms of crown acceleration and displacement have been noted for fixed base, linear SSI and nonlinear SSI. Three component nonlinear time history analysis has been performed to compare with one component time history analysis. Damage study of superstructure has also been performed.

TABLE OF CONTENTS

LIST OF FIGURE

LIST OF TABLES

1. INTRODUCTION

1.1 General

To study the soil structure interaction and its impact on seismic response of structures, extensive study has been performed over last three decades or so. Finding effect of soil structure interaction on nuclear containment structures is essential as the failure of structure can be very much detrimental to environment. The soil structure interaction is important in structural engineering since massive structures such as nuclear structures or dams are constructed on soft soils

1.2 Why it was necessary to study Soil- Structure interaction?

In Earthquake engineering, soil structure interaction is one of the most widely studied phenomena. It is important because vibrational behavior of structures during earthquakes can be influenced significantly by the properties of soil and the structure.

The nature of subsoil influences the response of structure constructed on it. Various past experiences proves the influence of nature of subsoil. In 1976 Tangshan, China earthquake, 50% of the building on thick soils were flattened to ground, whereas only 12% of the buildings on rock subsoil totally collapsed. Spitak earthquake 1988 struck in a sparingly populated part of Caucasus Mountains, causing destructions in villages close to epicenter. But the destruction on much larger scale occurred 25km to the south of the epicenter. Similar effects were reported for San Fernando, California earthquake (1971), Loma Prieta, California earthquake (1989) , Northridge , California earthquake (1994), Bhuj earthquake (2000) etc. But certain studies clearly indicate contradictory evidence on the effect of foundation soils on dynamic structural response. For example, more brick buildings were damaged on firm soils in Kanto earthquake in 1923. In Mexico city, there was a comparatively high damage rate of reinforced concrete buildings of 13 to 16 storeys founded on soft soils during 1957 earthquake. These studies clearly show that damage

due to shaking on different soil depends not on soil conditions only, but on the relation between the dynamic characteristics of the structure and soils beneath the structure.

As the energy demand is increasing, use of nuclear energy has increased all over the world, so there is construction of large number of nuclear power plant all over the world.

With more number of nuclear power plants, more is the concern for safety, because any structural damage to these structures can lead to threat of radiation, health hazards and environmental hazard as well. Earthquake can cause catastrophic structural damage to nuclear reactors. Out of operating nuclear power plants, about one fifth plants are placed in seismically active zones. In India, existing and proposed nuclear reactors are situated in seismic zone II and III, hence robust modeling techniques and design methodologies should be used for nuclear plant structures situated in seismic regions.

So, the conclusion drawn out of previous studies shows that in order to predict realistic response of given structure at given site, dynamic soil structure interaction should be given a fair importance while analyzing the structure.

1.3 What is soil structure interaction?

When light weight structure is built on very hard soil or rock, an assumption of input motion is same as free field motion of earthquake is valid. But, when massive structure rests on relatively soft soil, then the input motion at the base foundation of structure is significantly different than the free field motion.

Free field motion and fixed base structures

Ground motions that are not influenced by the presence of structure are called as free field motions. Structures founded on rock are considered as fixed base structures. When a structure founded on solid rock is subjected to an earthquake, the extremely high stiffness of the rock constrains the rock motion very close to the free field motion.[1]

Dynamic Soil structure interaction

When the structure is resting on soft soil deposit, the motion of the base of the structure to deviate from the free field motion due to the inability of the foundation to conform to the deformations of the free field motion. Also deformation of supporting soil takes place due to the dynamic response of the structure itself. This process, in which the response of the soil influences the motion of the structure and the response of structure influences the motion of soil, is named as soil structure interaction.

These effects are more significant for stiff and/ or heavy structures supported on relatively soft soils. The effects are small when soft and /or light structures founded on stiff soil. [1]

Degree of Influence of SSI

The degree of Influence of SSI on response of structure depends on the following factors[1]

1. Stiffness of soil.

2. Dynamic Characteristics of structure itself

3. Mass and stiffness of structure.

Basically the dynamic soil-structure interaction consists of two interactions, namely, kinematic interaction and inertial interaction.

Kinematic interaction

Seismic waves travel through the soil media during earthquake, discontinuity in the soil media is encountered at the interface of soil and foundation. Due to change in the properties of material scattering, reflection, refraction of seismic waves take place at the interface. So different nature of wave is observed at the interface as compare to what would have been observed without the presence of foundation and structure. At interface, as foundation is rigid as compare to soil, seismic wave cannot deform the way it would have deformed, so slippage of foundation takes place at the interface. This is a nonlinear phenomenon. Due to kinematic constraint imposed by the rigid foundation, rigid foundation acts like low pass filter by averaging out high frequency components in seismic motions.

The effects arising out of this interaction are called as *kinematic interaction effects*. The actual seismic input to the structural foundation is the result of kinematic interaction analysis considering only the geometrical and stiffness properties of structural foundation and soil.[2]

Inertial interaction

The soil structure interaction associated with the mass of structure is called as inertial interaction. Due to dynamic movement of structure during earthquake, inertial forces are generated which produces overturning moment and transverse shear. If the soil below foundation is compliant, then the dynamic displacement of soil takes place because inertial forces are transmitted dynamic forces to the foundation.

Linear and Nonlinear Soil structure interaction

Linear behavior of soil is valid for very small level of strains. Deformations induced by a seismic motion in soil can easily reach the limit of its linear elastic domain. Nonlinearity significantly influences the behavior of structure-foundation soil system. Direct approach and Beam-on Nonlinear Winkler foundation (BNWF) are the models take into account the nonlinear behavior of soil.

1.4 Objective of study

The seismic response of containment structure of an NPP has been investigated considering soil-structure interaction. Various issues like earthquake excitation, nonlinear modelling of containment structure with its reinforcement, depth of embedment, absorbing boundaries of the soil, nonlinear modelling of the soil and their effects on the response of containment structure have been studied. Following analyses are carried out for the study.

i) To perform fixed base analysis of structure.

ii) To perform linear soil-structure interaction.

iii) To study effect of soil-structure interaction on period of structure.

iv) To perform non-linear soil structure interaction.

v) To study response of structure in terms of acceleration and displacement at different locations

vi) To compare the response of structure with and without consideration of soil-structure interaction.

vii) To study response of structure to three component earthquake excitation with nonlinear SSI

viii) To study damage pattern in structure subjected to different earthquakes.

1.5 Organization of the dissertation

This dissertation report has 5 chapters. Chapter 1 introduces topic and specifies objective of study. Chapter 2 is related to past research done on the related topic. Chapter 3shows the analytical modelling of nuclear containment structure and soil beneath. Chapter 4 discusses results obtained from time history analysis with and without considering linear-nonlinear soil-structure interaction. Chapter 5 states the conclusion obtained from performed studies.

2. PAST RESEARCH

Housner (1960) studied soil structure interaction effects on nuclear reactors, indicated theoretically the effect of foundation rocking on structural response [3]

Newmark and Hall (1969) analyzed the behavior of NPP facilities with soil structure interaction (SSI). The effect of site amplification and soil foundation interaction on response is studied.[3]

Cheng (1995) studied use of infinite elements. He concluded that when gravity process is turned on, vertical displacement should not be restrained at infinite nodes in order to take into account the vertical stresses generated at these nodes due to gravity, and in subsequent analysis, vertical displacement should be restrained.[4]

Venancia (1997) used sub-structure and frequency domain methods to investigate effect of dynamic SSI on seismic NPP response. He provided equations for dynamic SSI for rigid foundation as well as equations for frequency domain analysis of MDOF systems. Conclusion drawn was quality of results depends mainly upon soil properties and adequate evaluation of structure. [5]

Ghiocel and Ostadan (2007) studied seismic ground motion incoherency effects on SSI response of NPP structures. This paper shows effect on ground motion incoherency on axisymmetric nuclear structures' seismic SSI response.. Stochastic and deterministic approaches are used to include incoherency. Additional rocking and torsional effects are examined due to incoherency. In high range frequencies incoherency effects are high as compare to low frequency ranges.[6]

Kawasato et al. (2008) studied experimentally Soil-Structure Interaction using large geotechnical centrifuge system. SSI is performed on hard rock with main focus on embedment effects and basement uplifts. Three vibration tests are performed , 1^{st} is shaking test for steel building using exciter settled on building with which impedance functions of soil are evaluated.2^{nd} is shaking table tests which is performed on soil having

cavity, by which reduction effect of motion is confirmed for cavity of soil. 3rd is shaking table test for steel building, by which uplift and embedment effects are confirmed. Soil spring stiffness and frequency increases with embedment. Radiation damping also increases with increase of embedment. Also it is seen that uplift response of building decreases with increase in embedment, and it becomes remarkable with increase in frequency.[7]

Raychowdhury and Hutchinson (2009) evaluated the performance of a nonlinear Winkler-based shallow foundation model using centrifuge test results.

In this paper, winkler model consists of nonlinear inelastic springs, gap elements, dashpots. Backbone of these springs is checked with shallow foundation experiment. Model is evaluated with the help of number of centrifuge experiments. Experiment includes Square and strip footing, bridge models, building models, sand and clay on which footings rest, static and dynamic loading, aspect ratios. It has been observed that model can predict responses like moments, shear, rotation, settlements reasonably. Hysteresis shape of moment-rotation curves, shear- sliding curves and settlement-rotation curves are captured reasonably. Due to lack of coupling between vertical and horizontal modes of response, model underestimates sliding demands.[8]

Saxena, Paul and Kumar (2010) studied the effects of slip and separation on seismic SSI response of nuclear structure. They modeled nuclear structure with soil-structure interface which allows slip and separation. Joint elements used to model interface have proper joint stiffness calculated. The material taken is linear for reactor and soil and interface is considered elastoplastic. This study shows that slip and separation cause increase in stresses at certain points depending upon coefficient of friction. Also, as the response depends upon the stiffness of interface, finding proper joint element stiffness is important.[9]

Bolisetti, Whittaker (2011) studied seismic Structure-soil-structure interaction of NPP structures. The effect of SSSI in pair of nuclear structures is compared with individual structures. Both NPP are studied for in-plane and antiplane alignments. For separation distance and relative masses, the frequency transfer functions are calculated at different locations of reactor. Three cases are studied, 1st is pair of standard reactors, 2nd is pair of

heavy reactors and 3rd is one standard and one is heavy reactor. For each case three analysis is done for three separation distances. El centro earthquake motion is used for analysis. Study showed that SSSI effects are high for rocking frequencies of reactor. Four fold increase in mass of standard reactor did not make much difference in response for same separation. But response is significantly affected when standard and heavy reactors are placed.

Bhaumik and Raychowdhury (2012) studied seismic response of Nuclear power plant structure with nonlinear Soil-structure interaction. The inelastic behavior of soil is captured by beam on nonlinear winkler foundation model. The internal shear wall is studied for its seismic response. Response is measured in terms of forces and displacement demand using IDA. Reduction in base shear and moments observed and increase in drift, ductility is also observed. Sliding and settlement increased by consideration of nonlinear SSI with increase in intensity of ground motion.[10]

Saxena and .Paul (2012) studied effects of embedment considering the slip and separation on seismic SSI response of nuclear structure. They modeled soil, structure and soil-structure interface. Due to slip and separation redistribution of stresses take place at the soil and structure near the interface. Time domain analysis has been carried out to take into account nonlinearity of problem. This study drew the following conclusions,[11]

- Horizontal slip decreases with increase in embedment, and is insignificant beyond 1/4th embedment.
- Vertical separation also decreases with increase in embedment is significant till half depth embedment.
- Stress response also decrease with increase in embedment (especially tensile stress response), this decrement in stresses is significant till 1/4th embedment.
- Is is important to model interface after 1/8 embedment as bonded model (no interface modeled) underestimates the stresses generated.

Samangany, Naderi and Shahabi far (2013) did static and dynamic analysis of storage tanks for Soil-Structure interaction. Effect of SSI is studied and also effect of soft, medium and hard soil with SSI on response of tanks has also been studied. The study concludes

that stresses are high in walls as compare to floors, so crack check needs to be done for walls. Contact elements between raft and soil considerably changes the response of wall. In static and dynamic analysis, as soil become stiffer, pressure on walls increases. Interaction is more in case of soft soil as compare to hard soil. Horizontal displacement is more when soil is soft. It is concluded that it is better to avoid constructing tanks on soft soils.[12]

Bhaumik and Raychowdhury (2013) analyzed seismic response with nonlinear SSI of NPP structure. The analysis of internal shear wall of Indian NPP is done in open sees where interface is modeled with beam on nonlinear winkler foundation approach. The NPP rests on medium densed sandy silt soil. Push over analysis and cyclic analysis and also incremental dynamic analysis with 30 recorded ground motions are performed. Cyclic analysis showed that equivalent viscous damping increased up to two times upon consideration of nonlinear SSI. Pushover analysis showed that yield force may reduce till 22% and yield displacement can increase up to 46%. Incremental dynamic analysis showed that shear and moment demands at base decreased. This indicated SSI can lead to economic seismic design. Roof drift increased by 25%. Seismic demands of shear walls are sensitive to friction angle of soil and not much to unit weight

Kumar and Maheshwari (2013) studied SSI of NPP structure by finite element modeling. The study showed that nuclear structure response is high when it is situated on soft soil as compare to located on rock. Also as the embedment increases structure becomes stiffer and so time period decreases. Also responses are smaller when considered dampers as absorbing boundary of elastic half space media as compare to elementary boundaries due to reflection of waves.[13]

Kumar, Raychowdhury and Gundapalli (2015) studied seismic response of NPP with nonlinear winkler based approach for modeling soil-structure interface. Winkler nonlinear approach has distributed array of inelastic springs, gap elements and dashpots. 3D modelling is done which is subjected to bidirectional ground motion. This paper studies effect of nonlinear SSI and embedment effects. The study showed that time period increased by 10.4% due to nonlinear SSI. 24% reduction in base shear forces. Embedment

made system stiffer and thus decreased fundamental time period of structure. Rotation and sliding responses also decrease with increase in embedment.[3]

.

3. ANALYTICAL MODELLING

For the response study, following containment structure is taken for analysis.

3.1 Dimensions of Structure

The containment structure consists of cylindrical wall with hemispherical dome at top.

Dimensions [14]

Inner radius of containment structure = 18.9m

Inner radius of dome = 18.9m

Thickness of dome wall = 0.762m

Thickness of cylindrical wall= 0.915m

Depth of raft= 3m

Radius of raft= 43.6 m

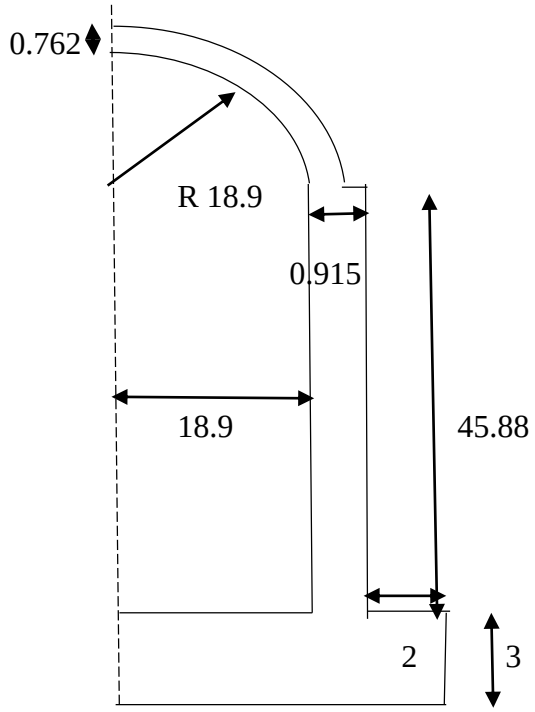

Fig 3.1 Dimensions of Containment Structure [14]

3.2 Reinforcement Details

Two layers of reinforcements are provided with clear cover of 40mm. Containment wall is provided with hoop and meridional reinforcement in two layers. One layer is near inside surface of containment and other is near outside surface of containment. For Cylindrical walls, all the reinforcement have 57mm dia @ 300mm c/c spacing. For hemispherical dome, up to half height double layer of hoop reinforcement and for above half single layer of hoop reinforcement are provided. Meridional reinforcement is also provided in double layer with rebar dia 43mm @ 300mm c/c spacing are provided in both meridional and hoop direction in dome portion of structure. For raft also on both the top and bottom surface 43mm dia rebars at 300m c/c spacing are provided in both horizontal directions. On vertical sides of raft also same reinforcement detail is provided.

Reinforcement of Dome

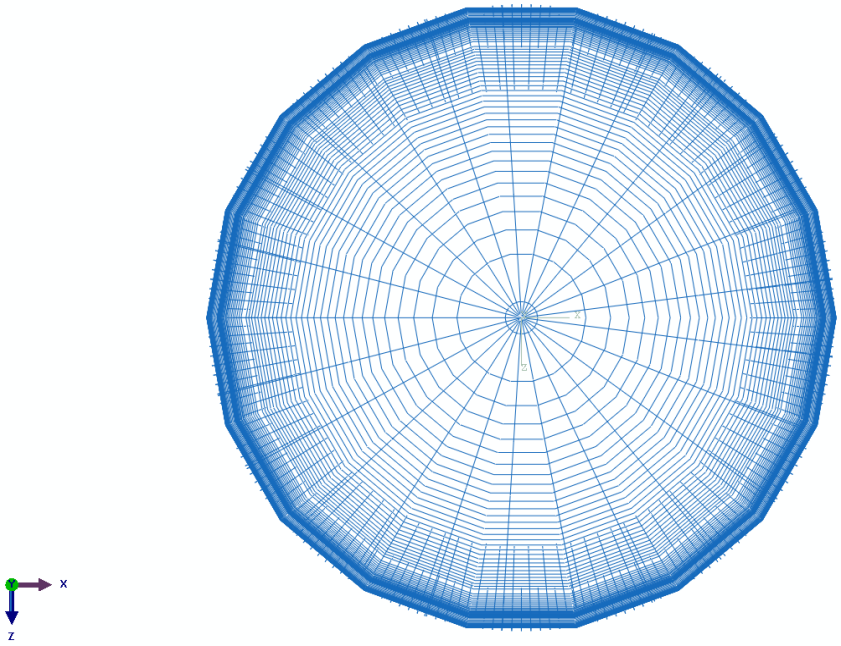

Fig 3.2 Dome Reinforcement (Top view) [14]

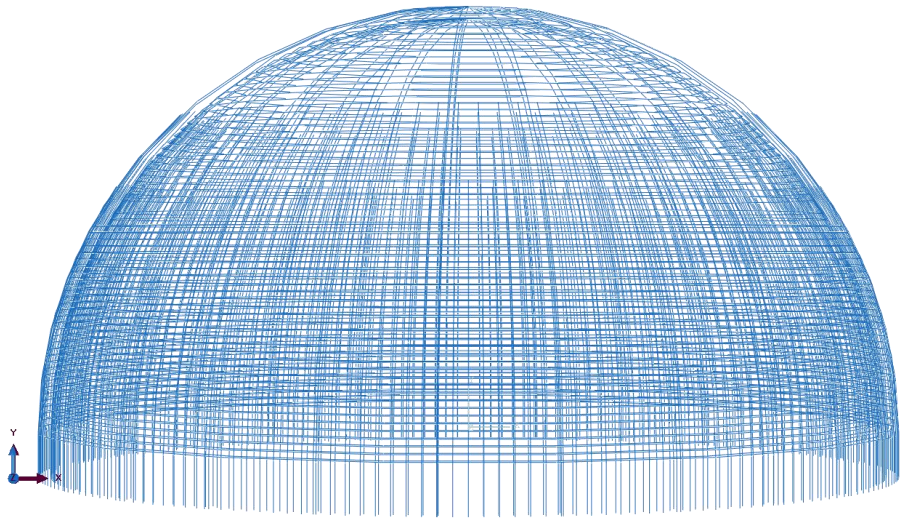

Fig: 3.3 Dome Reinforcement (Elevation) [14]

Cylindrical Wall Reinforcement

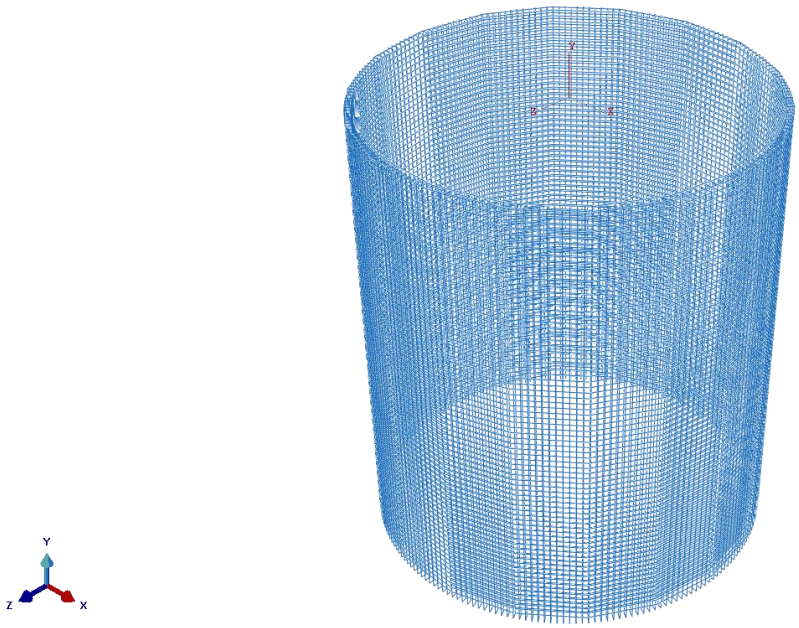

Fig 3.4 Cylindrical Wall Reinforcement [14]

Raft Reinforcement

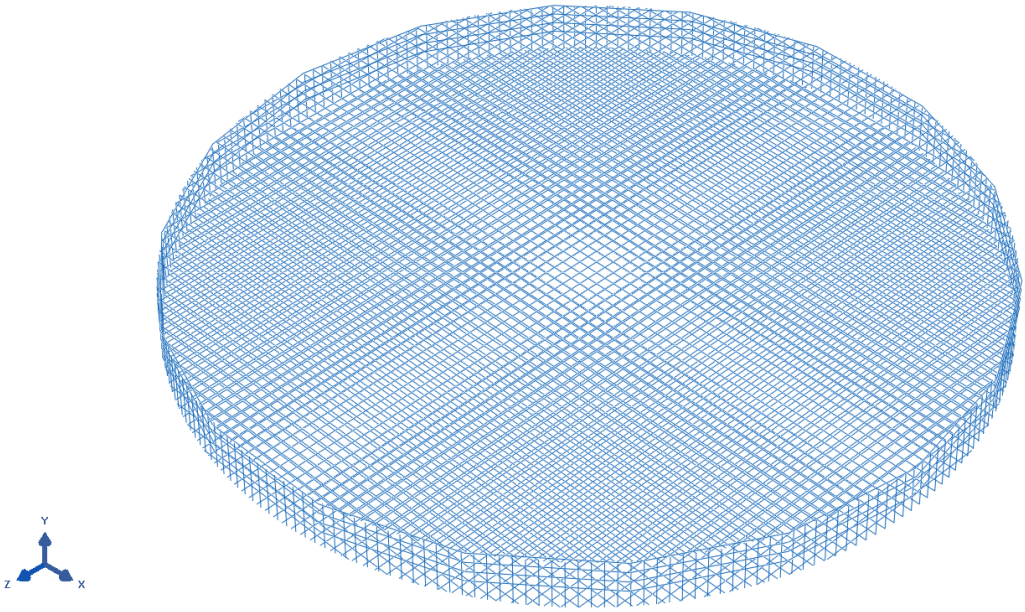

Fig 3.5 Raft Reinforcement [14]

3.3 Dimensions of Soil Block

Dimensions

The soil block taken for analysis has depth equal to 1.5 times the height of structure and the horizontal extent of soil from center of containment structure is 1.5 times the width of structure on either side of center. Soil block where truncated is provided with absorbing boundaries to simulate the infinite extent of soil with the help of *dashpot elements (ref.3.6)*

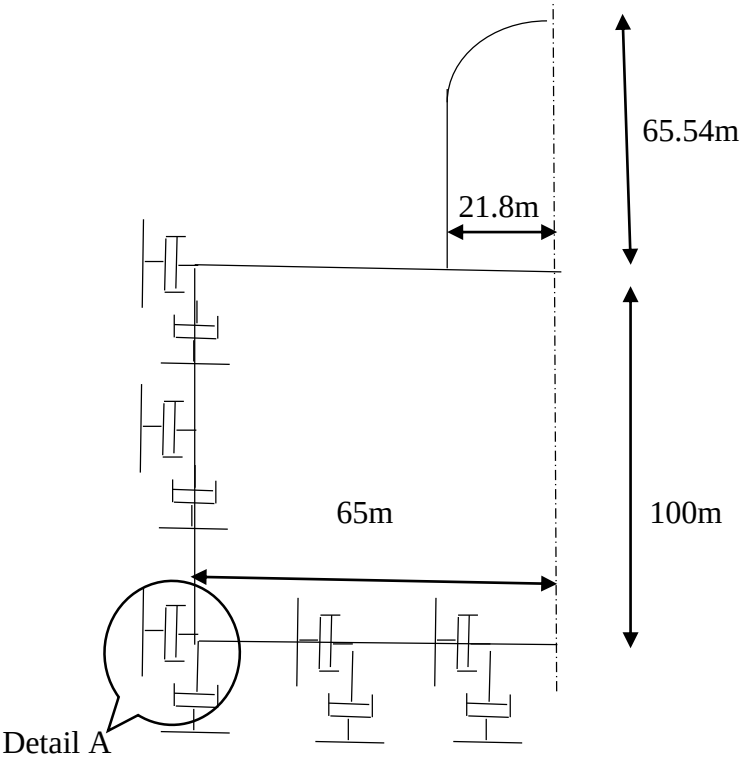

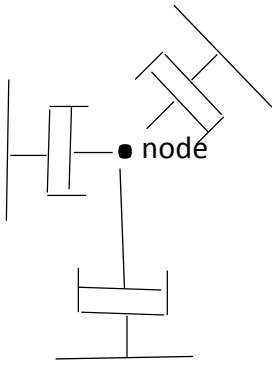

Detail A

Fig 3.6 Soil block details

3.4 3D Finite Element Model

Concrete is modeled with 8 nodded 3D elements (C3D8R) for both the cylinder and dome portion of containment structure. Reduced integration technique is used. 2 nodded truss elements are used to model reinforcement with the assumption of full bond between the reinforcement and the concrete.

Finite portion of soil is modeled with 8 nodded 3D (C3D8R) elements. Absorbing boundaries are represented with the help of dashpots. Each node has 3 dashpots

Convergence study

Superstructure

A total number of 6408 nodes and 3900 elements are used for *superstructure.* Convergence study is performed to arrive at these number of elements. For convergence study, first ten modal frequencies are compared. Following are the results for convergence study. Frequencies of all the ten modes for model having 5028 nodes almost match with the corresponding frequencies of model having 6408 nodes. Therefore the later has been adopted.

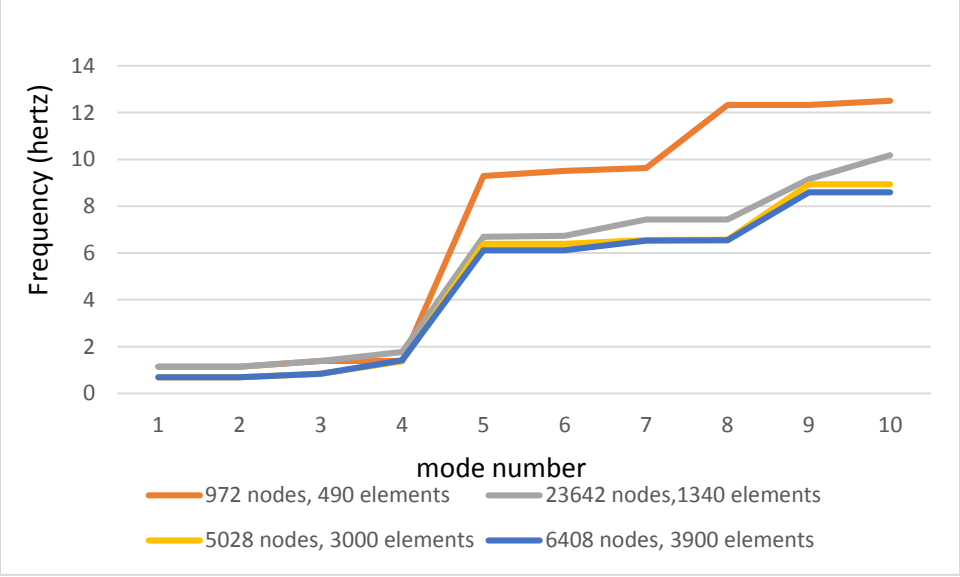

Fig 3.7 Convergence study- Superstructure

Soil

A total number of 5437 nodes and 4602 elements are used for *soil block.* Convergence study is performed to arrive at these elements. For convergence study, first four modal frequencies are compared. Following are the results for convergence study. Frequencies of all the four modes of the model having 35677 nodes almost match with the corresponding frequencies of the model having 5437 nodes. Therefore the later has been adopted.

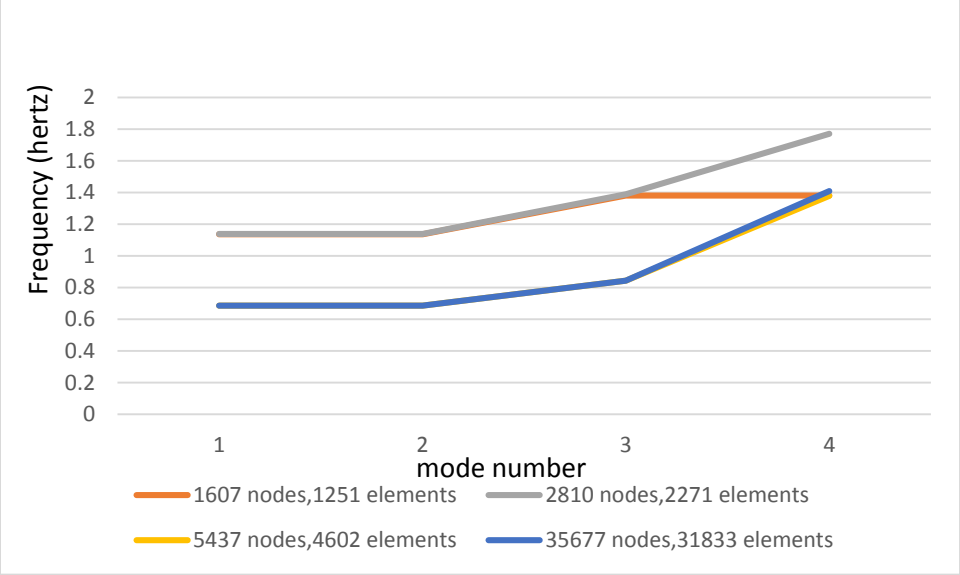

Fig 3.8 Convergence study-soil model

3D FEM model of nuclear structure and soil beneath

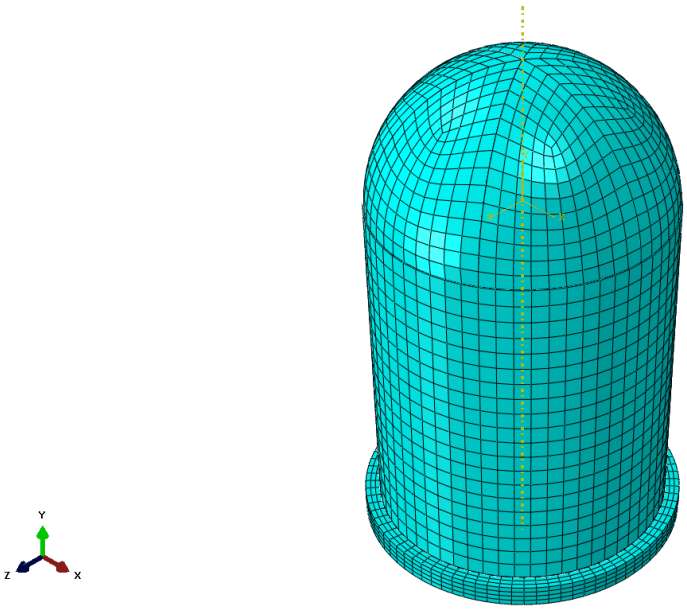

Fig 3.9 3D FEM model of Superstructure

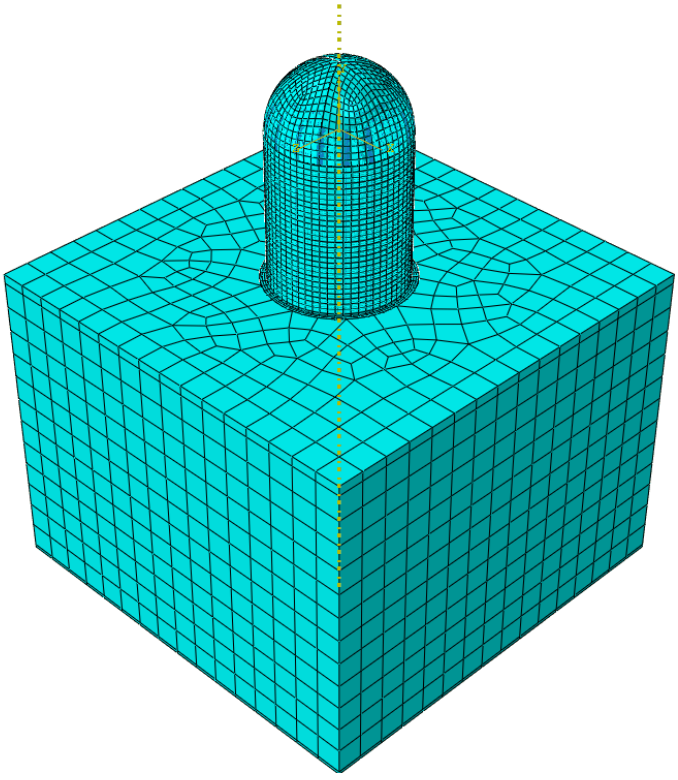

Fig 3.10 3D Fem Model of Structure and Soil

3.5 Modelling of Soil Structure interface

In present study, interface is of soil and structure has been provided with tie constraint.

3.6 Modelling of Unbounded Medium

Foundation soil is extended infinitely in all three directions. While modelling of soil, it is not feasible to model infinitely extended soil, therefore soil model has to be truncated at certain boundaries. It therefore necessitates that the boundary provided at truncated location should represent infinite extent of soil that means these boundaries should be able to absorb the earthquake waves in order to avoid trapping of energy in problem domain which could lead to wrong response analysis of structure to the seismic activity.

Absorbing boundaries can be provided by following procedures,

1. Elementary boundary
2. Local boundary
3. Consistent boundary
4. Infinite elements

Elementary boundary

The soil mesh is truncated at the artificial boundary, where zero displacement or zero surface traction is forced. These boundaries do not behave as absorbing boundaries and they perfectly reflect impinging waves.

Local boundary

Local boundaries are also called as viscous boundaries. P wave and S wave dampers are used at the nodes of the boundary. These dampers attempt to absorb the impinging wave,

Accuracy is not good for thin surface layers. There is no coupling of degree of freedom of the nodes located on artificial boundaries. Viscous dashpots are to be used at each node and each degree of freedom.

These type of boundary conditions are used in current boundary modelling in Abaqus. Dashpots are provided with proper damping coefficient C. C is calculated as follows,

$C = \rho \times A \times V_S$ ($or\ V_p$) ……[15]

$C =$ Force per unit relative velocity

$\rho =$ Mass density of soil

$A =$ Tributary area of damper

$V_s =$ Shear wave velocity

$V_p =$ Pressure wave velocity

Consistent Boundary

These boundaries can absorb all impinging wave irrespective of angle of incidence. So complete transmission of waves take place without reflection. These boundaries with considerable reduction in degree of freedom can be directly applied at the side of foundation. Here all degree of freedom are coupled.

Infinite elements

Infinite elements are used when small part is to be modelled as compared to surrounding media. So, the infinite soil can be modelled taking small part of soil using infinite elements. Infinite elements are only linear elements. In static continuum analysis it provides stiffness, in dynamic analysis it maintain the previously stressed state. So, during dynamic analysis no displacement of these elements occur. These elements provide normal and shear tractions which proportional to normal and shear component of velocity. This assures transmission of earthquake waves. During dynamic analysis, these elements does not provide stiffness but maintains initial stresses so, no displacement takes place but rigid body motion can take place. But it is usually very small**.**[15]

3.7 Material Modelling

3.7.1 Concrete Damage Plasticity Model [15]

For nonlinear properties of concrete, concrete damage plasticity model has been used. The concrete damaged plasticity model is provides a capability for the analysis of concrete structures under cyclic and dynamic loading. Concrete behaves brittle under low confining pressure. It cracks in tension and crushes under compression to ensure failure. The constitutive theory in this section captures the effects of irreversible damage of concrete occurs with the failure under low confining pressures.

Main features of the concrete damaged plasticity model are given below.

Strain rate decomposition

$$\varepsilon' = \varepsilon'^{el} + \varepsilon'^{pl}$$

ε' is the total strain rate, *el* is for elastic part of the strain rate, and *pl* is for plastic part of the strain rate.

Stress-strain relations

The stress-strain relations are by scalar damaged elasticity

$$\sigma = (1 - d)D_0^{el} : \varepsilon - \varepsilon^{pl}$$

D_0^{el} is the undamaged initial elastic stiffness of the material;

$D_0^{el} = (1 - d)D_0^{el}$ is the degraded elastic stiffness;

d is the scalar stiffness degradation variable, (d=0 undamaged to d = 1 fully damaged material).

Damage related with the failure mechanisms of the concrete makes in a reduction in the elastic stiffness.

Damage and stiffness degradation

The hardening variables $\epsilon_t^{\sim pl}$ and $\epsilon_c^{\sim pl}$ are first considered for uniaxial loading conditions and then used for multiaxial conditions.

Uniaxial conditions

It is assumed that the uniaxial stress-strain curves can be converted into stress- plastic strain curves

$\sigma_t = \sigma_t\ (\epsilon_t^{\sim pl}, \dot{\epsilon_t}^{\sim pl}, \theta\ , f_i)$

$\sigma_c = \sigma_c\ (\epsilon_c^{\sim pl}, \dot{\epsilon_c}^{\sim pl}, \theta\ , f_i)$

The subscripts *c* is for compression and *t* denotes tension

$\dot{\epsilon_t}^{\sim pl}$and $\dot{\epsilon_t}^{\sim pl}$ are the equivalent plastic strain rates,

$\epsilon_t^{\sim pl} = \int_0^t \epsilon_t^{\sim pl}$ = are the equivalent plastic strains,

$\theta$is the temperature,

f_i, (i = 1, 2, …) are other predefined field variables

The effective plastic strain rates under uniaxial loading conditions are given as,

$\dot{\epsilon_t}^{\sim pl} = -\dot{\epsilon_{11}}^{\sim pl}$in uniaxial tension

$\dot{\epsilon_c}^{\sim pl} = -\dot{\epsilon_{11}}^{\sim pl}$in uniaxial compression

Let σ_c is a positive quantity representing the magnitude of the uniaxial compression stress;

$\sigma_c = -\sigma_{11}$

As shown in Fig 3.9, at any point of softening branch the concrete is unloaded. The elastic stiffness of the material is degraded. The degradation of this stiffness is considerably different between tension and compression tests, the effect is more prominent in both the cases when the plastic strain increases. The degraded response of concrete is given uniaxial damage variables,

$$d_t = d_t\left(\tilde{\epsilon}_t^{pl}, \theta, f_1\right), (0 \leq d_t \leq 1)$$

$$d_c = d_c\left(\tilde{\epsilon}_t^{pl}, \theta, f_1\right), (0 \leq d_c \leq 1)$$

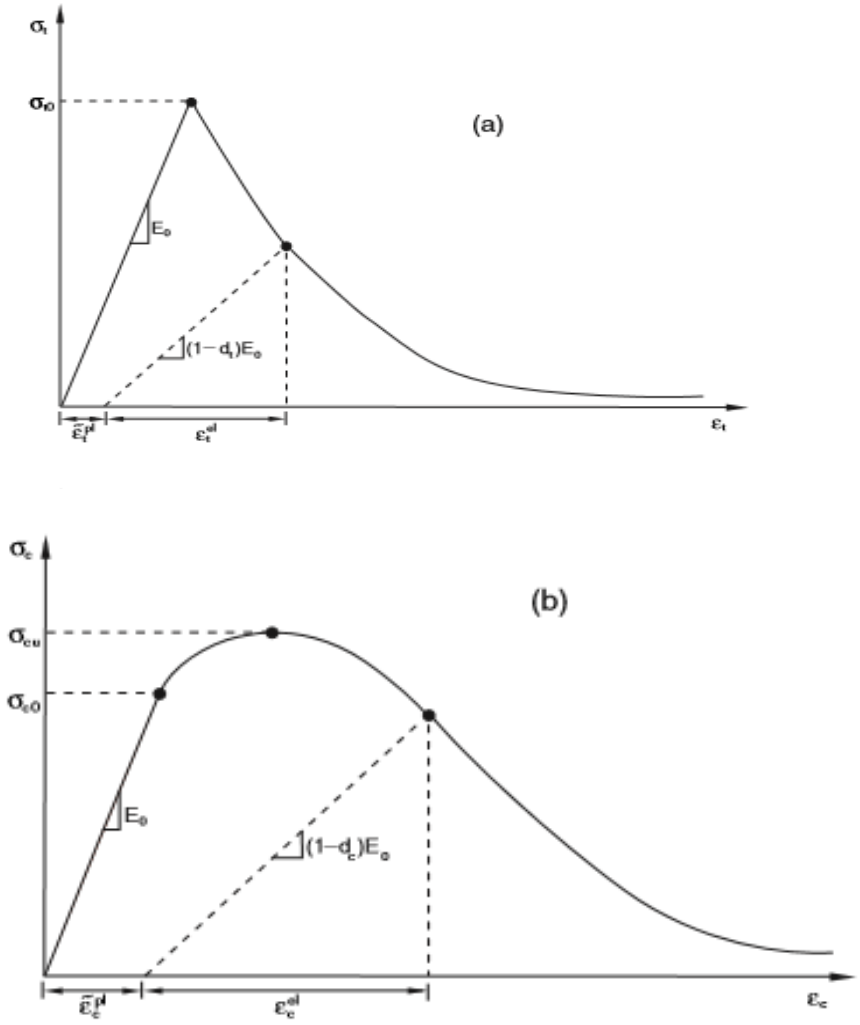

.Fig 3.11 Uniaxial loading response of concrete tension (a) and compression (b)

If E_0 is the undamaged initial elastic stiffness of the material, the stress-strain relations under uniaxial tension and compression loading are, respectively as follows

Uniaxial cyclic conditions

Under uniaxial cyclic loading conditions the opening and closing of previously formed micro-cracks, as well as their interaction takes place. It is observed from experiments that there is some recovery of the elastic stiffness when load changes sign in cyclic loading. The effect is more as the load changes from tension to compression, causing tensile cracks to close, recovers of the compressive stiffness.

This model assumes that the reduction of the elastic modulus is given by scalar degradation variable, *d*, as

This expression is for both in the tensile and compressive sides of the cycle. Abaqus assumes,

$$(1-d) = (1-s_t d_c)(1-s_c d_t)$$

where s_t and $s_c = 0$ represent stiffness recovery effects.

$$s_t = 1 - w_c r(\sigma_{11}) \; ; 0 \leq w_t \leq 1$$

$$s_c = 1 - w_c[\,1 - r(\sigma_{11})] \; ; 0 \leq w_c \leq 1$$

$$r\,(\sigma_{11}) = H\,(\sigma_{11}) = 1 \; if \; \sigma_{11} > 0$$

$$= 0 \; if \; \sigma_{11} < 0$$

The weight factors w_t and w_c are material properties, which control the recovery of the tensile and compressive stiffness.

Figure shows Uniaxial load cycle (tension-compression-tension)

Stiffness recovery factors: $w_t = 0$ and $w_c = 0$

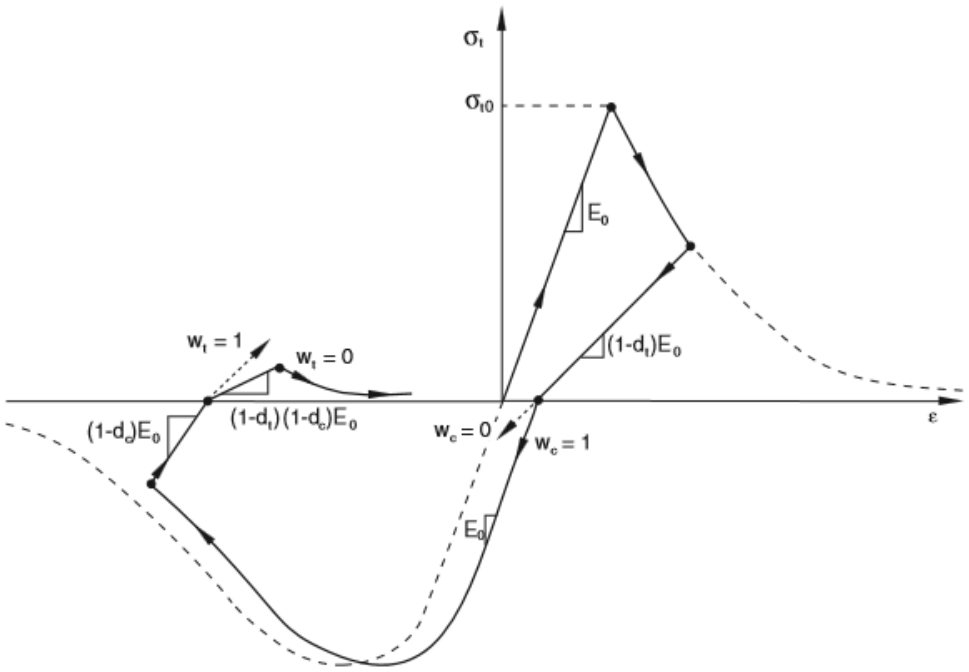

Fig 3.12 Uni-axial load Cycle (Tension –compression-tension), $w_t = 0$ and $w_c = 0$

3.7.2 Nonlinear Modelling of Soil

Soil mechanics for a long time has been based on Hookes law of linear elasticity for stress and strain analysis. As per the usual practice soil can be modelled as

1. Elastic under workable load

2. Perfectly plastic under ultimate failure condition

3. Perfectly visco-elastic under long term loading.

Mohr-Coulomb failure criteria [16]

The Shear strength of soil is defined by shear stress on failure plane. It is necessary to find the failure plane. For this purpose triaxial test can be performed in laboratory. Mohr circle can be drawn from sample stress by using known values of principle stresses. A series of Mohr circles can be plotted from the tests carried out on different samples. A tangential line to Mohr circles define Mohr-coulomb envelope.

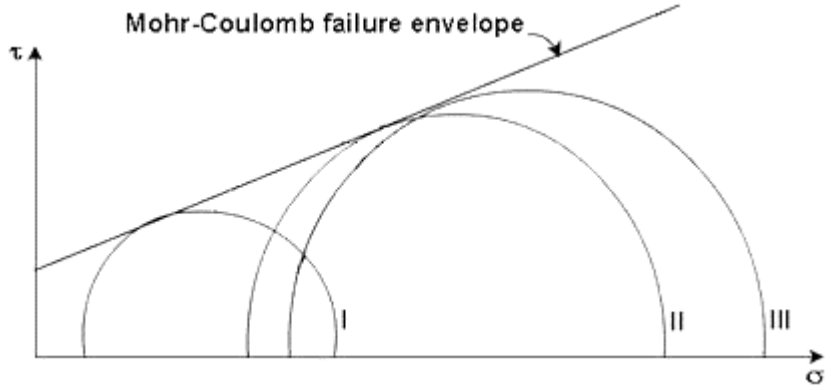

If Mohr circle of any other soil sample lies below the failure envelope, every plane in the sample experiences less shear stress than the shear strength of sample. Therefore, point of tangency gives fair idea about inclination of failure plane. Orientation of plane can be determined by pole method.

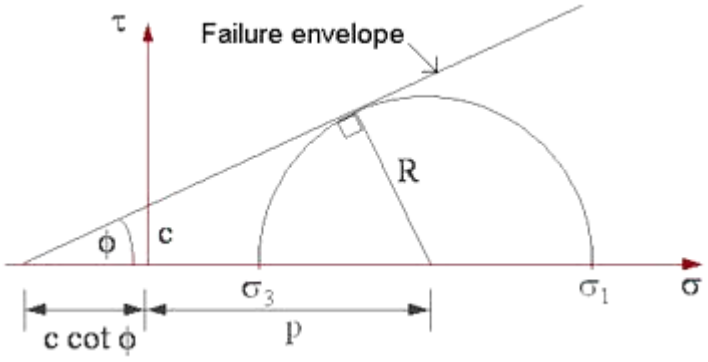

The Mohr-Coulomb failure criterion represented in equation as,

$\tau_f = c + \sigma_f tan\emptyset$

τ_f = Shear Stress on the failure plane

c = cohesion

σ_f = normal stress on the failure plane

f = angle of internal friction

The failure criterion can be represented in the form of the relationship between the principal stresses. From the geometry of the Mohr circle,

$$\sin\theta = \left[\frac{\frac{(\sigma_1 - \sigma_3)}{2}}{c\ cot\emptyset + \frac{(\sigma_1 + \sigma_3)}{2}}\right]$$

Rearranging,

$$\sigma_1 = \sigma_3\left(\frac{1 + sin\theta}{1 - sin\theta}\right) + 2c\sqrt{\left\{\frac{(1 + sin\theta)}{(1 - sin\theta)}\right\}}$$

3.7.3 Material Properties

Damping

Concrete = 5%, Soil = 15%

Concrete [17]

Table 3.1 Concrete Damage Plasticity Parameters

Material Properties	**Values**
Density (kg/m^3)	2400
Young's Modulus (GPa)	24.80
Poisson Ratio	0.20
Dilation Angle	38
Flow Potential Eccentricity	1
Biaxial to uniaxial stress failure ratio fbo/fc	1.12
Shape of loading surface in deviatory plane	0.67

Stress, strain and damage coefficient in compression

Concrete compression hardening		Concrete compression damage	
Stress (Mpa)	Crushing strain	Compression damage coefficient	Crushing strain
15	0	0	0
20.197	7.47E-05	0	7.47E-05
30	9.88E-05	0	9.88E-05
40.303	0.000154	0	0.000154
50.007	0.000762	0	0.000762
40.236	0.002558	0.195402	0.002558
20.236	0.005675	0.596383	0.005675
5.257	0.011733	0.894865	0.011733

Stress, strain and damage coefficient in tension

Concrete tension stiffening		Concrete tension damage	
Stress (Mpa)	Cracking strain	Tension damage coefficient	Cracking strain
1.99893	0	0	0
2.842	3.33E-05	0	3.33E-05
1.8698	0.00016	0.406411	0.00016
0.862723	0.00028	0.69638	0.00028
0.226254	0.000685	0.920383	0.000685
0.056576	0.001087	0.980093	0.001087

Reinforcement

Table 3.2 Material Properties of steel

Material properties	Values
Density (kg/m3)	7830
Young's Modulus (Gpa)	200
Poisson's ratio	0.3

Stress-strain relation of steel

Stress (Mpa)	Plastic Strain
500	0
520	0.018
600	0.038
650	0.058
650	0.098

Soil [18]

Table 3.3 Mohr-coulomb soil model used in abaqus

Soil Parameters	**Values**
Density (kg/m^3)	2000
Young's Modulus of elasticity (Mpa)	680
Poisson's Ratio	0.3
Angle of internal friction	35
Angle of dilation (assumed)	20
Cohesion (Kpa)	200

4. RESULTS AND DISCUSSIONS

4.1 Validation of concrete damage plasticity (CDP) model

To validate the CDP model of Abaqus the lab results of 3 point bending single edge notched concrete beam is compared with the one modeled in software. Following diagram shows the geometry of specimen. Dimensions mentioned are in millimeters. Beam thickness is 100mm.

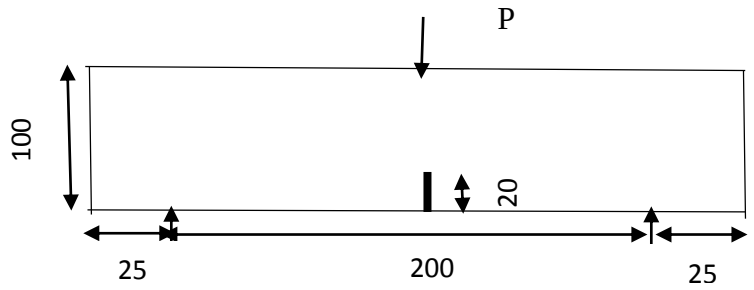

Fig 4.1 Three Point Beam Dimensions [17]

The finite element mesh used to discretize the beam is shown in following figure.

No of elements are 5708

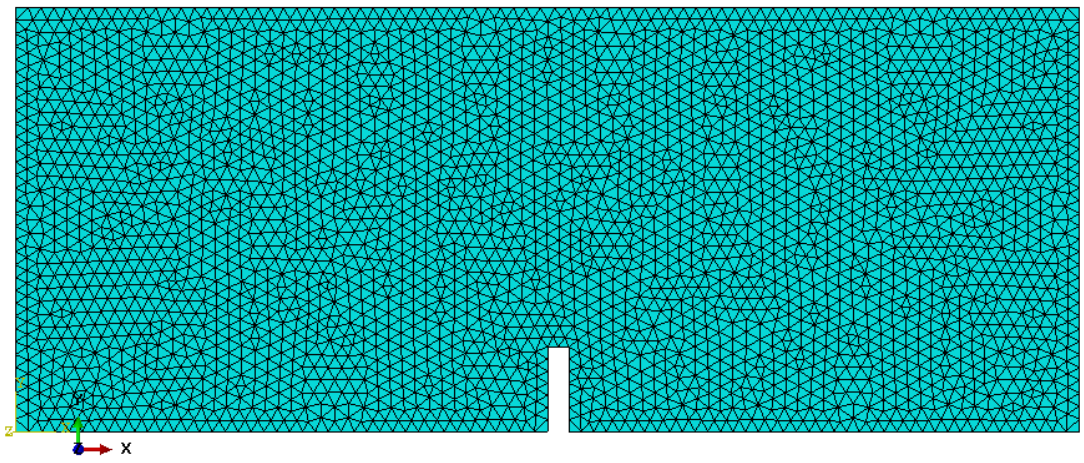

Fig 4.2 2D Fem Model of Beam

Following is the crack pattern obtained from software analysis

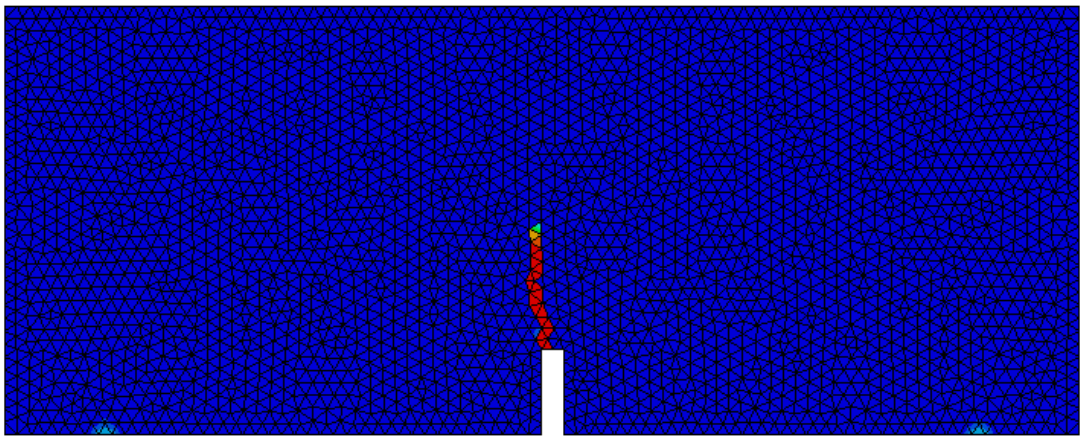

Fig 4.3 Crack Pattern from Software

Crack pattern obtained in lab experiments

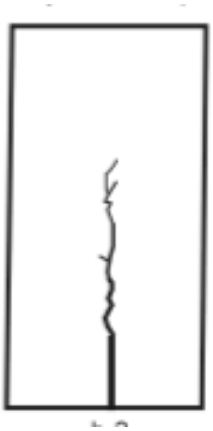

Fig 4.4 Crack Pattern obtained in Lab[17]

The obtained crack pattern from Abaqus software using CDP model is similar to crack pattern obtained in laboratory. Comparison of results is shown below.

In this concrete three point bending beam specimen single dominant crack pattern is obtained. The crack obtained in the experiment presented by Davies 1996, is similar to that of obtained from software analysis.

Comparison of experimental and numerical results

For this crack pattern, following results are obtained.

Experimental: Load 5.22 KN for B38

Numerical: Load 8KN for B50

This successful comparison validates the concrete damage plasticity model of Abaqus finite element program.

4.2 Validation of 3D modelling

A frequency analysis is considered for validation of three dimensional analysis in Abaqus. Shinozuka et al. have analyzed the containment structure having cylindrical wall and hemispherical dome on the top.[14] The containment structure has been assumed fixed at base. The dimensions are same as described before. Finite element model is made in Abaqus with same dimensions and frequency analysis is performed. Comparison of results is shown below.

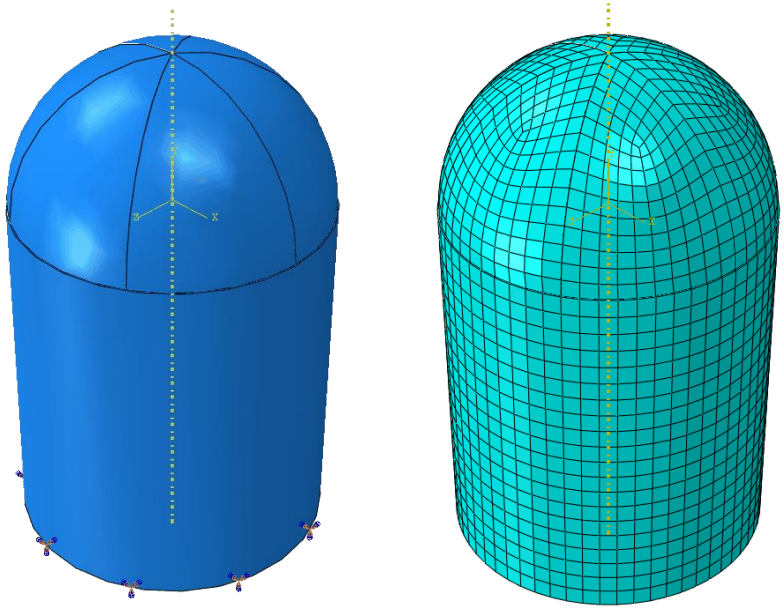

Fig 4.5 Present 3D Fem Model in Abaqus

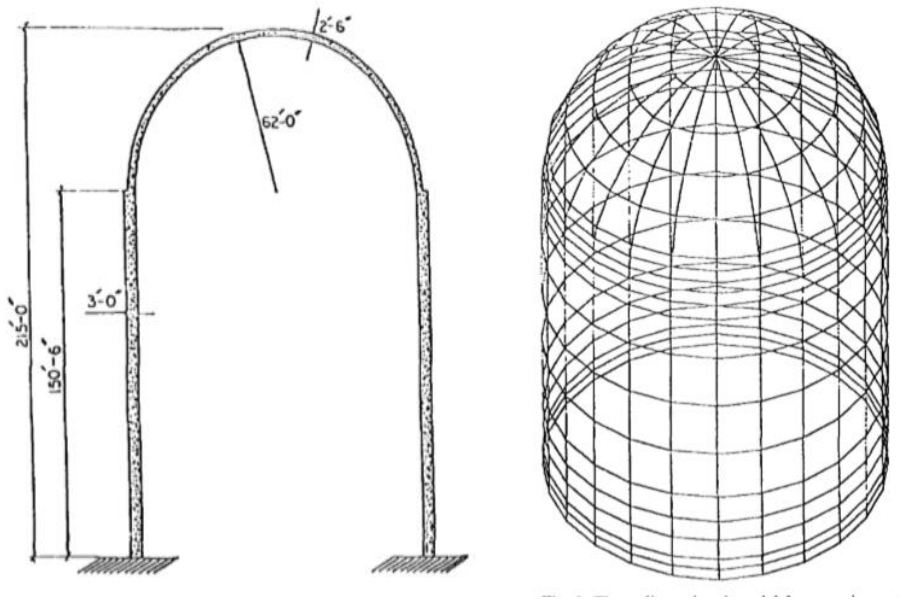

Fig 4.6 Cross section and 3D model made by author [14]

Table 4.1 Comparison of Frequency Analysis Results

Mode No.	Frequency (Cycles/s)	
	Present Study	Shinozuka et al. (1984)
1	4.176	4.196
2	4.176	4.196
3	5.264	5.541
4	5.267	5.541
5	6.348	6.676
6	6.353	6.676
7	6.437	6.794
8	6.437	6.794
9	8.689	9.076
10	9.220	9.776

As results of analysis matches with the author's analysis. Hence 3D modelling of abaqus is validated.

4.3 Comparison of Fundamental time period of structure with and without Soil

Structure is analyzed for finding frequencies of initial 4 modes. Firstly it is provided with fixed supports at the base of raft, and the result obtained is compared with the structure provided with soil beneath.

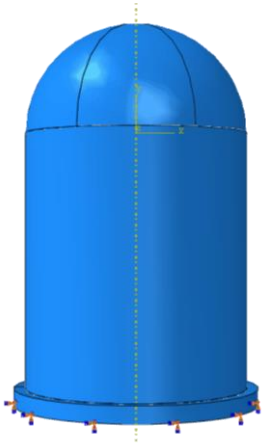

1st mode frequency =4.108 sec-1
Fundamental period = 0.24 sec

Fig.4.7 3D model showing fixity at raft

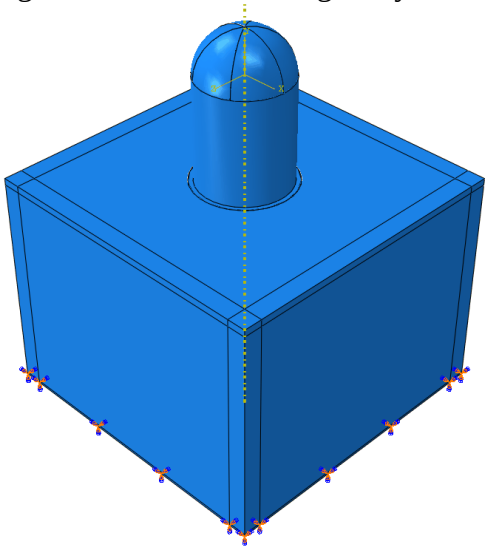

1st mode frequency= 2.25 sec-1

Fundamental period = 0.44 sec

Fig. 4.8 3D model showing soil below the structure

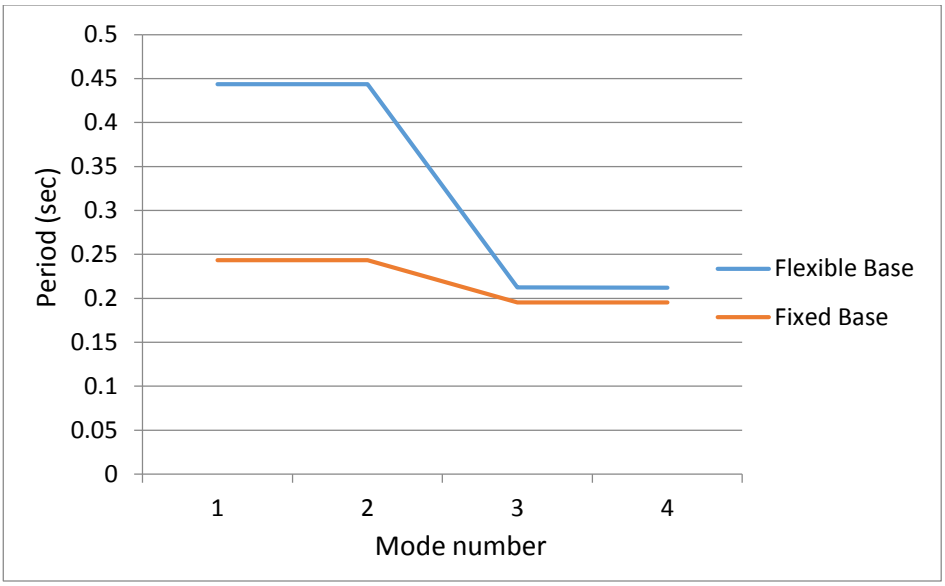

Fig. 4.9 Effect of soil-structure interaction on natural period

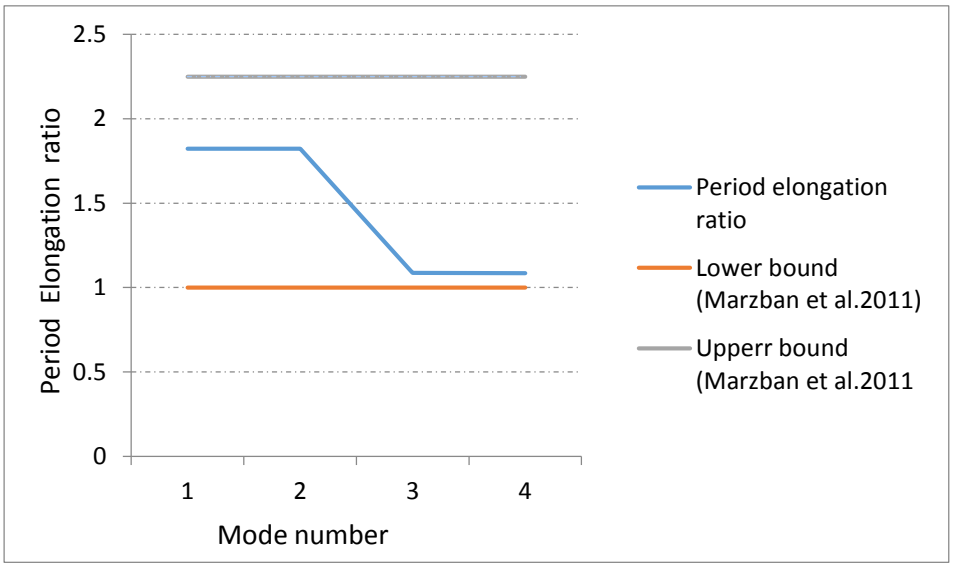

Fig. 4.10 Elongation of period

Above charts shows that period elongation takes place upon incorporation of soil-structure interaction. This elongation takes place because flexibility is induced at the base of foundation due to movement of soil. Fig 4.10 shows that maximum elongation takes place in fundamental modes as compare to higher modes. The elongation of period in all the modes is within range as specified by Marzban et.al, which states that depending upon soil characteristics period ratio varies between 1 to 2.25 [19]

4.4 Validation of Soil Model-Absorbing Boundaries

For validation of soil modelling, acceleration in the form of sine wave has been applied at the base of soil. Two cases have been compared to understand the effect of absorbing boundaries achieved with the help of dashpots. Initially elementary boundary conditions are used at the truncated soil boundary. Side boundaries are provided with vertical rollers and horizontally retrained boundary conditions, base of soil is fixed in both vertical and horizontal directions. The results obtained from this case are compared with soil model provided with dashpots on the side boundaries as well as at the bottom of soil.

Case1: Elementary Boundary Conditions

Acceleration at the base of soil

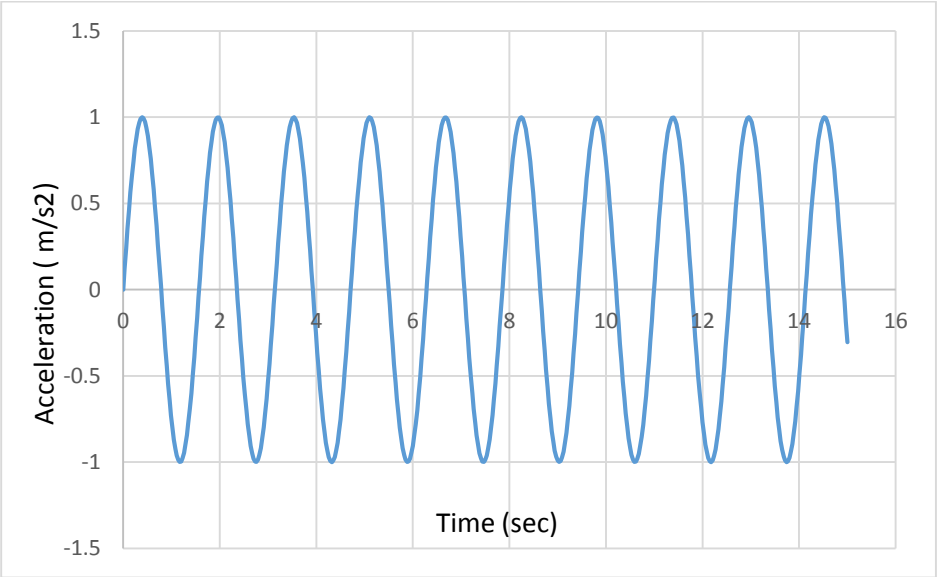

Fig. 4.11 Acceleration at the base of soil for elementary boundary condition

Acceleration at the top of soil

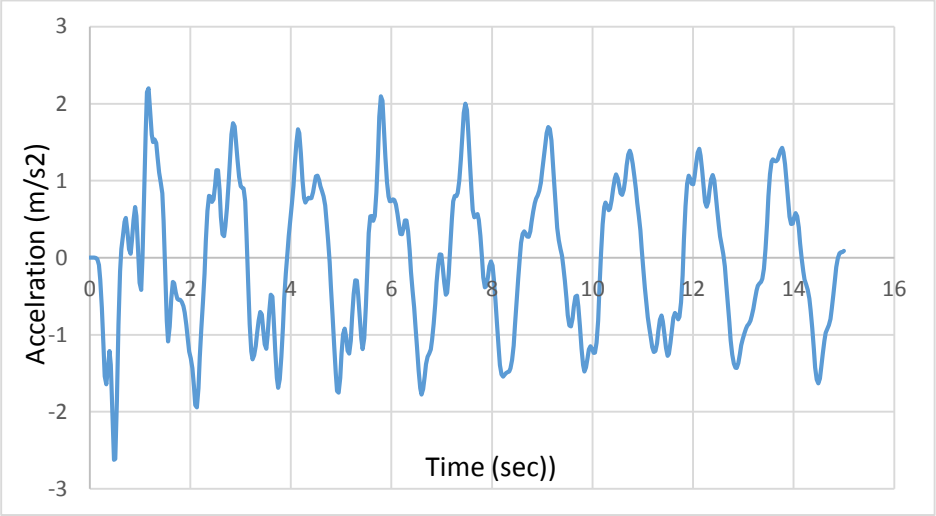

Fig. 4.12 Acceleration at the top of soil for elementary boundary condition

Case 2 : Absorbing Boundaries-Dashpots

Acceleration applied at the base in this case is same as it was applied in elementary boundary condition. The acceleration recorded at the top soil is shown below

Acceleration at the top of soil

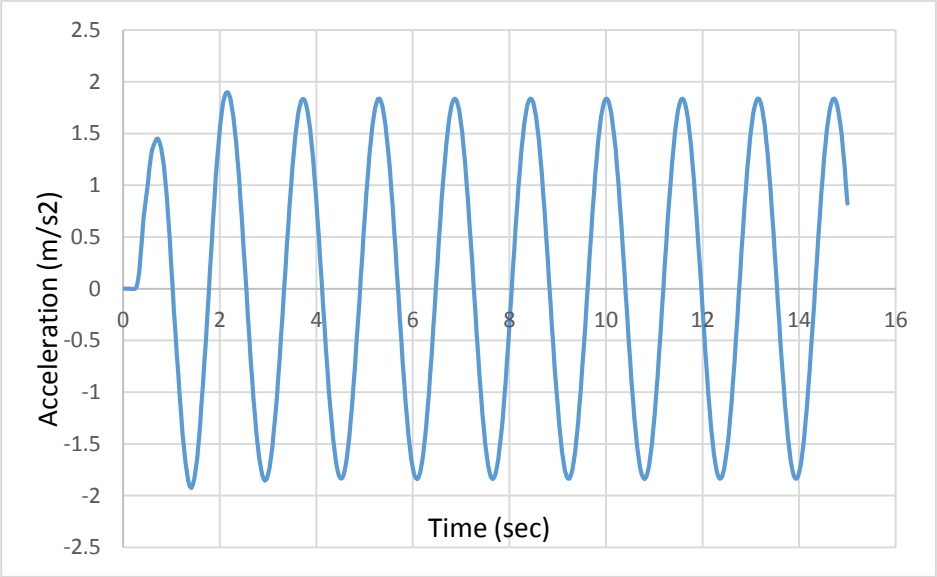

Fig. 4.13 Acceleration at the top of soil for absorbing boundaries

In Fig. 4.12, the waves are reflected back from the boundary in problem domain. That is the reason behind the variation in the pattern of sine wave appears. In Fig. 4.13, because of absorbing boundaries in the form of dashpots, pattern appears to be a sine wave. It implies that the boundary absorbs the waves as intended.

4.5 Validation of Absorbing Boundaries with Deepsoil software

Acceleration applied at the base of soil is shown in Fig. 4.11. Acceleration history is measure at the top of soil in Abaqus as well as in Deepsoil software.

Acceleration at the top of soil

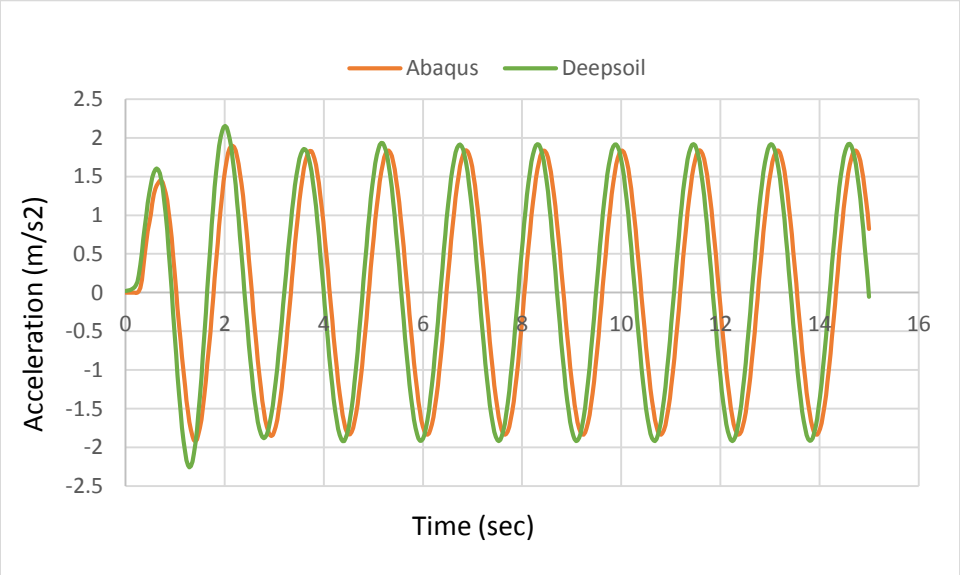

Fig. 4.14 Comparison of Abaqus and Deepsoil outputs

Fig 4.14 shows that, amplification obtained in abaqus model is almost same as obtained with deepsoil software. In Abaqus, soil is meshed for finite element modelling whereas in case of Deepsoil, elastic halfspace theory is used to represent soil. Therefore the marginal difference obtained in the acceleration response.

4.6 Time History Analysis

The acceleration time history record of Northridge earthquake (1994), Loma Prieta earthquake (1989) and Kobe (1995) are selected for seismic analysis of containment structure with and without soil. Considering IS code response spectra, Spectrum compatible time-history is generated for zone V for hard soil. So, the PGA of horizontal acceleration time history is taken as 0.36g for MCE as mentioned by IS code. Before performing time history analysis, gravity analysis has been done, and the stresses induced due to gravity are prescribed as initial stress condition prior to dynamic analysis.

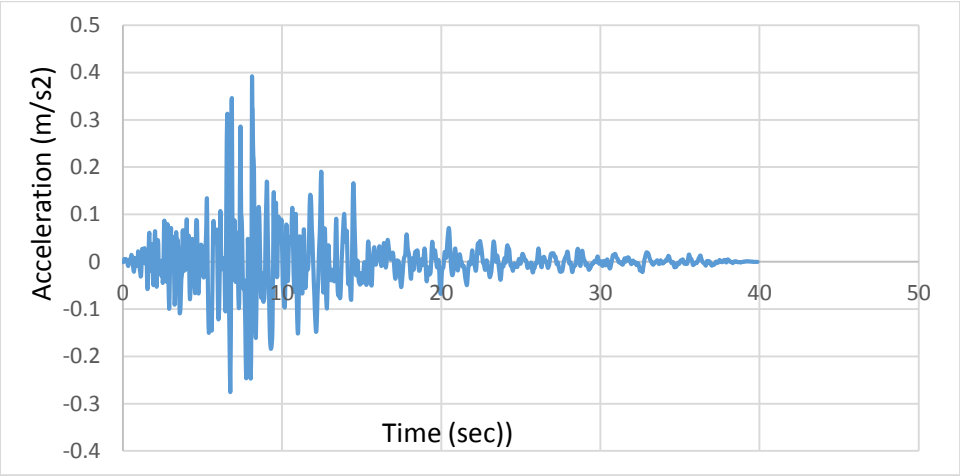

Fig 4.15 Acceleration Time History of Northridge Earthquake

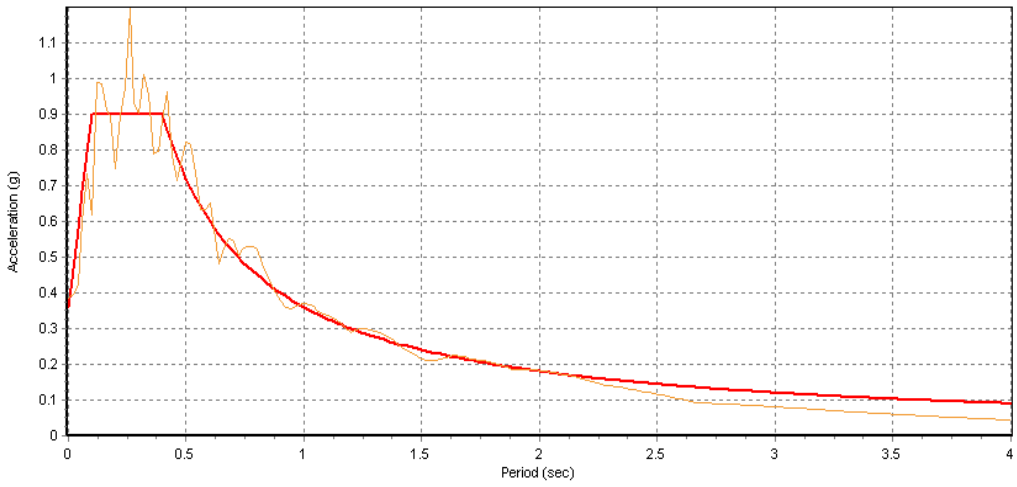

Fig 4.16 Matched response spectra for Northridge earthquake

The spectrum compatible time history for Northridge is shown in Fig 4.15. 'Seismomatch' software is used for matching response spectra. The obtained response spectra is plotted against target response spectra shown in fig.4.16.

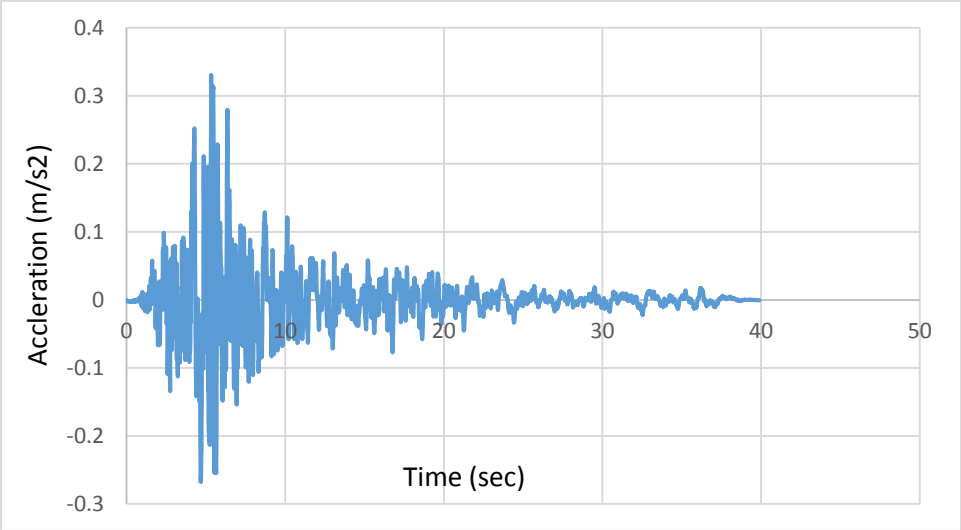

Fig 4.17 Acceleration Time History of Loma-Prieta Earthquake

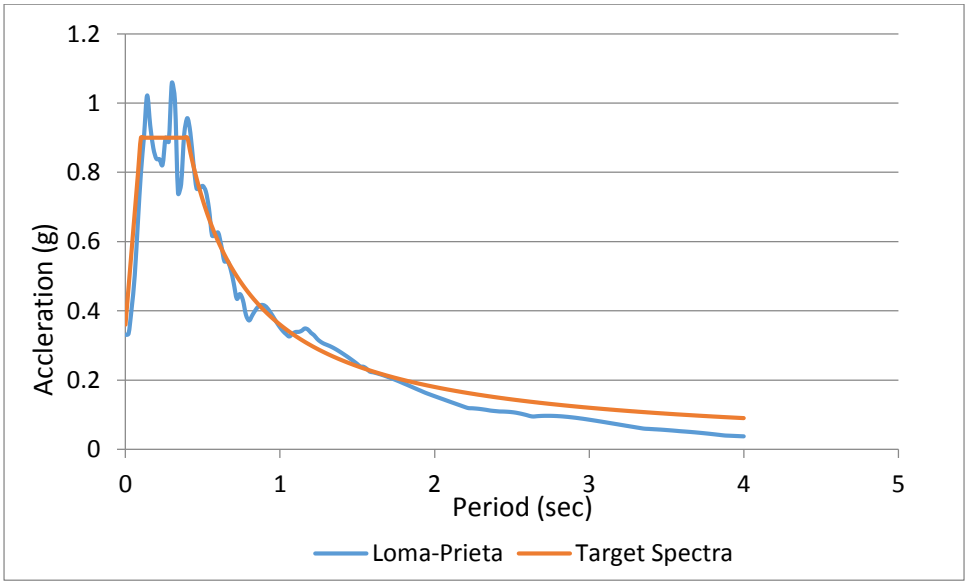

Fig 4.18 Matched response spectra for Loma-Prieta earthquake

The spectrum compatible time history for Loma-Prieta is shown in fig 4.17. The obtained response spectra is plotted against target response spectra shown in fig.4.18.

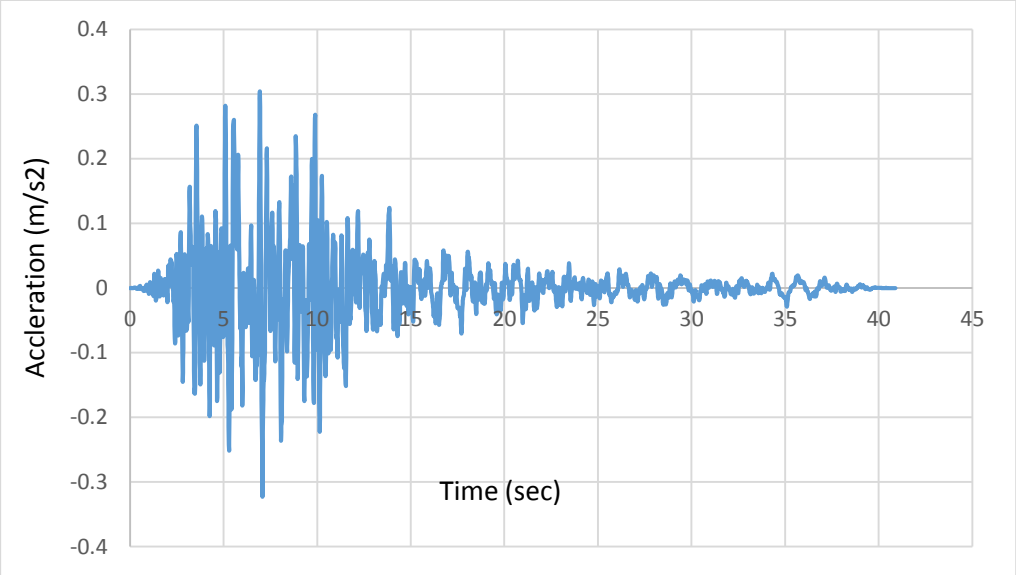

Fig 4.19 Acceleration Time History of Kobe Earthquake

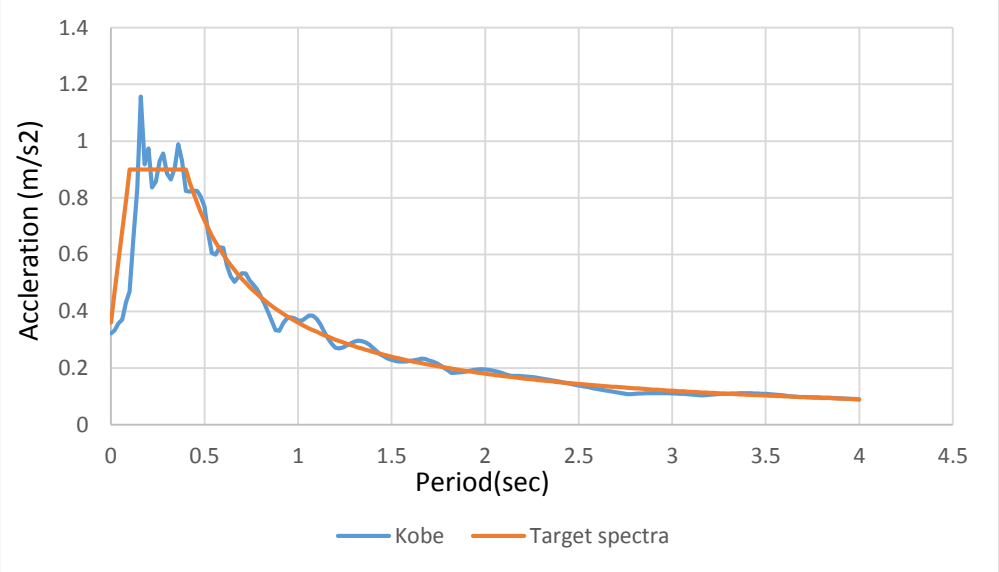

Fig 4.20 Matched response spectra for Kobe earthquake

The spectrum compatible time history for Kobe is shown in Fig 4.19. The obtained response spectra is plotted against target response spectra shown in Fig.4.20.

Estimation of Input Motion

The above mentioned time history cannot be applied directly at the base of soil model,i.e 100m depth, considered here. So, the outcrop motion has to be deconvoluted to get the response at the base of soil. Following Flowchart shows the various steps of deconvolution process[20]

Motion at Rock Outcrop (Time domain)

↓ (Fast Fourier Transformation)

Motion at the rock outcrop (Frequency Domain)

↓ Compute the transfer function and multiply)

Motion at the base of the foundation (Frequency Domain)

↓ (Inverse Fast Fourier transform)

Desired Motion at the base of soil/rock (Time domain)

The transfer function depends on shear wave velocity, depth, damping of soil and impedance ratio. For consideration of soil-structure interaction, input motion is applied at the base of soil. Following figure proves necessity of deconvolution. Deconvolution generally provided less peak amplitude as compare to peaks obtained at rock outcrop motion.

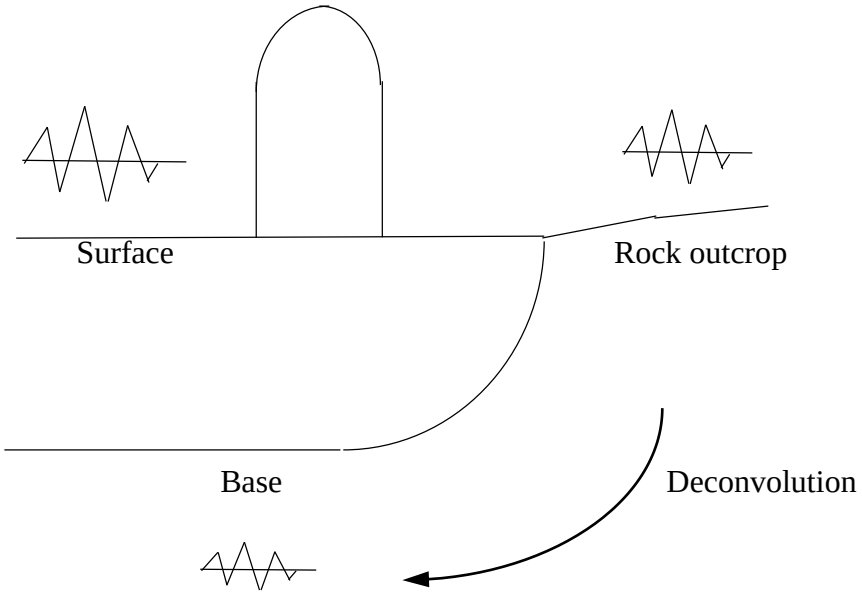

Fig 4.21 De-convolution of Motion

Following time histories are deconvoluted time histories. The peak value of the acceleration of Northridge earthquake is reduced to 0.29g from 0.36g PGA at the outcrop. Peak value of acceleration of Loma-Prieta is reduced to 0.26g from 0.36g PGA. Peak value of acceleration of Loma-Prieta is reduced to 0.27g from 0.36g PGA. These motions are applied the base of soil model to obtain response of structure. For deconvolution 'DEEPSOIL' software has been used.[21]

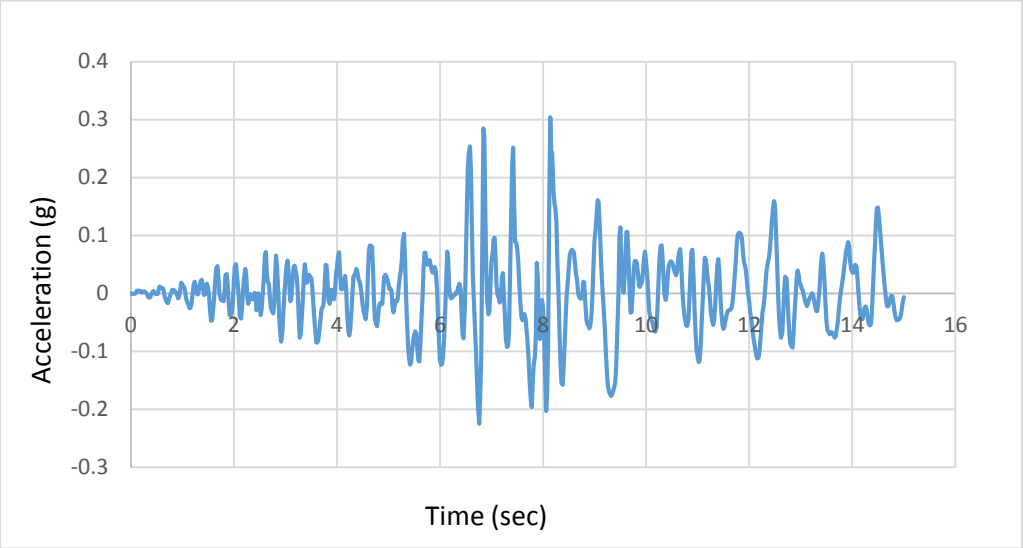

Fig 4.22 De-convoluted Northridge Earthquake Motion

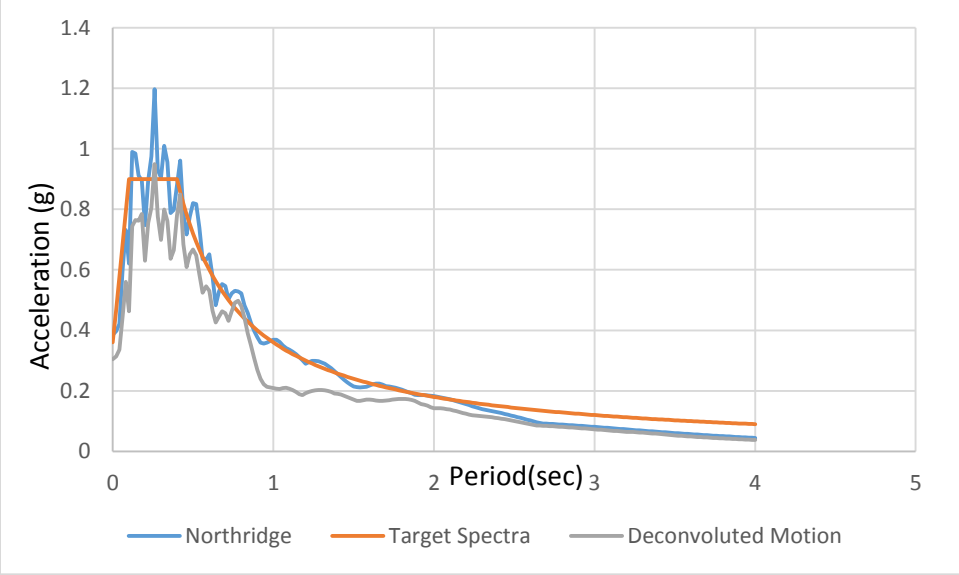

Fig 4.23 Comparison of response spectra for Northridge Earthquake

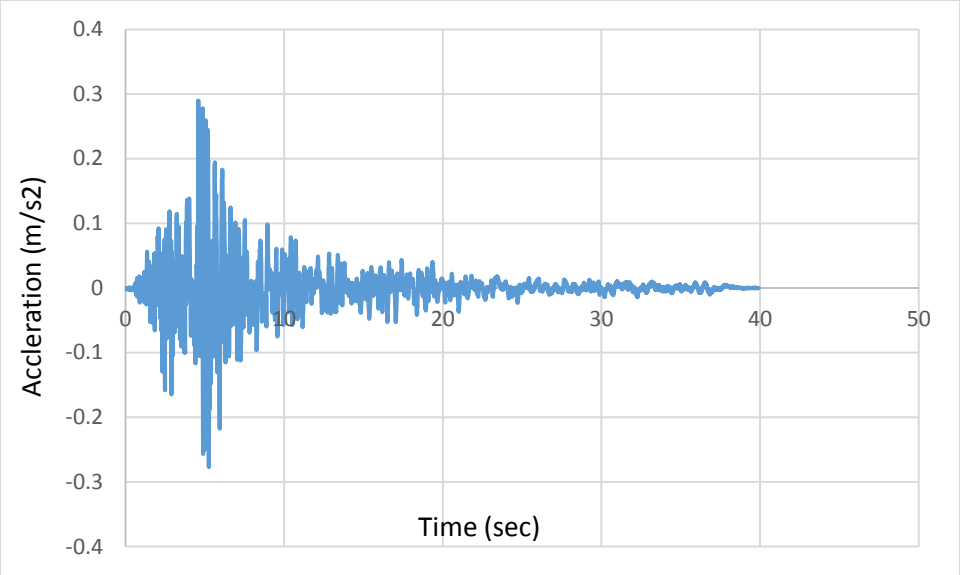

Fig 4.24 De-convoluted Loma-Prieta Earthquake Motion

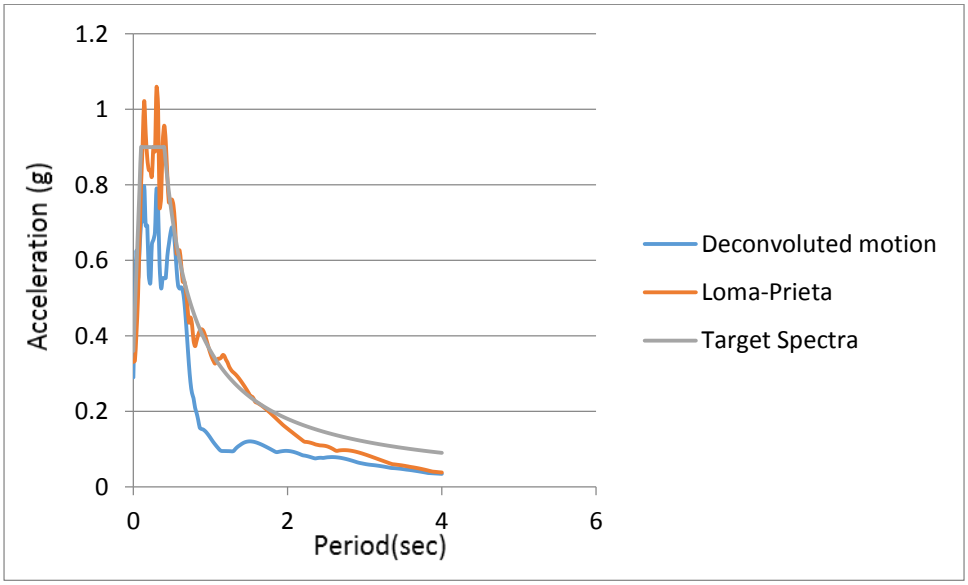

Fig 4.25 Comparison of response spectra for Loma-Prieta Earthquake

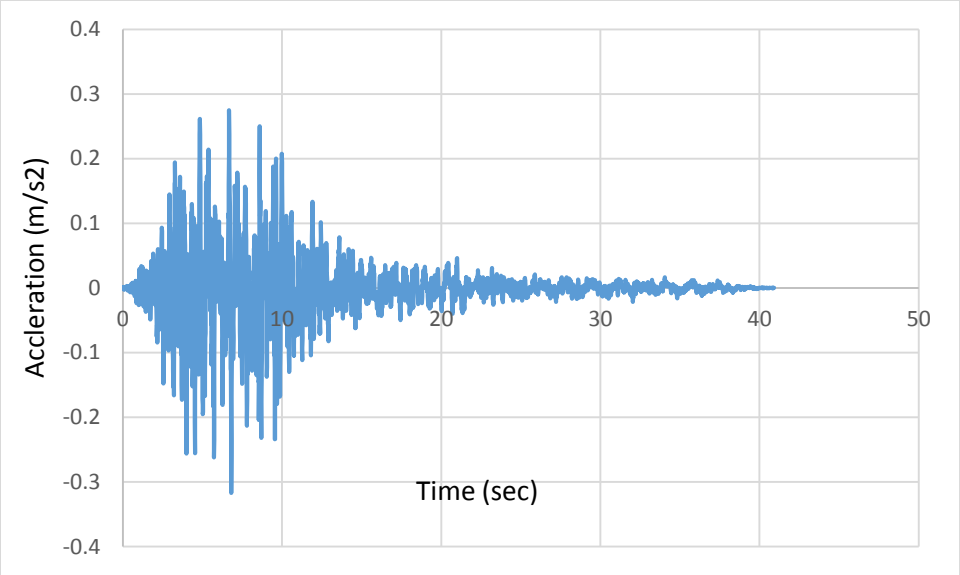

Fig 4.26 De-convoluted Kobe Earthquake Motion

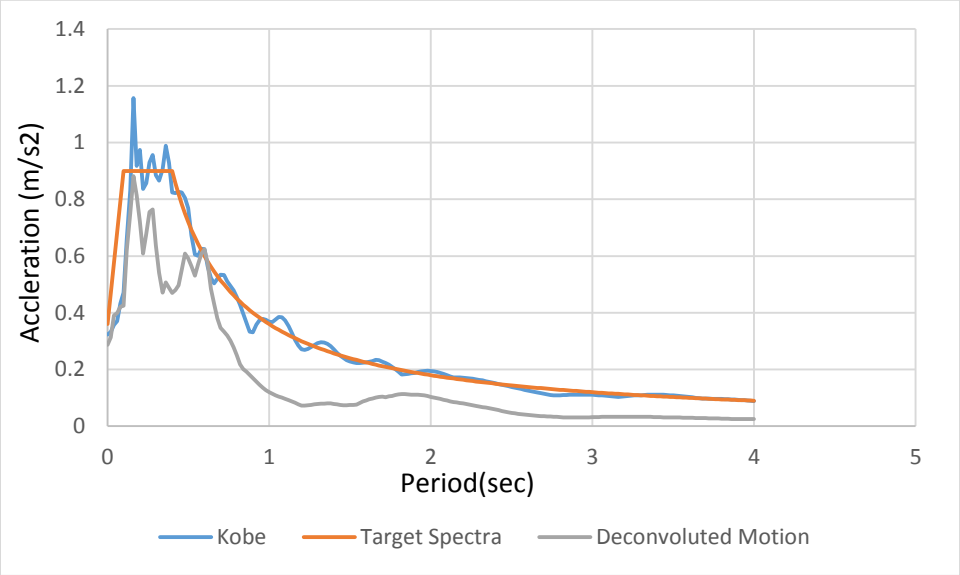

Fig 4.27Comparison of response spectra for Kobe Earthquake

4.6.1 Results of Northridge Time History Analysis

Analysis is done for finding the response of nuclear containment structure in terms of acceleration and displacement. Results are obtained at soil top (below raft) and at crown. Comparison of results obtained in following three cases is done.

Case1: Fixed base analysis

Case2: Linear soil-structure interaction analysis

Case3: Nonlinear soil-structure interaction analysis

Case 1: Fixed Base Time history Analysis of Structure

Acceleration time history at the base of raft

It is the time history obtained at the surface of soil after performing ground response analysis of rock outcrop motion considering nonlinear properties of soil.

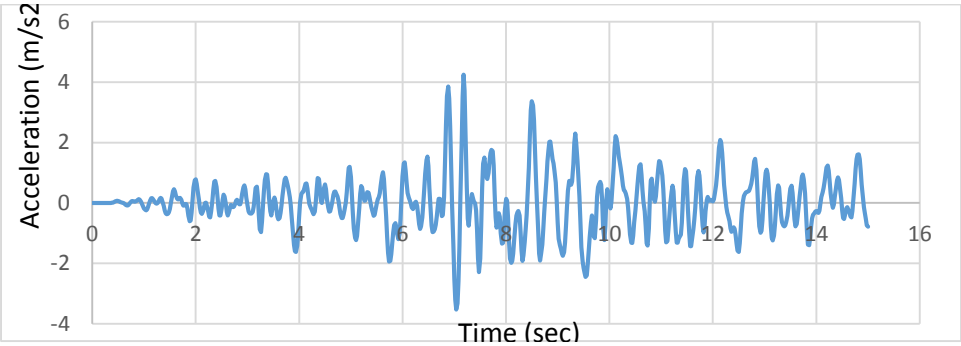

Max acceleration = 0.43g

(a) Acceleration time history at raft bottom

Acceleration recorded at the crown

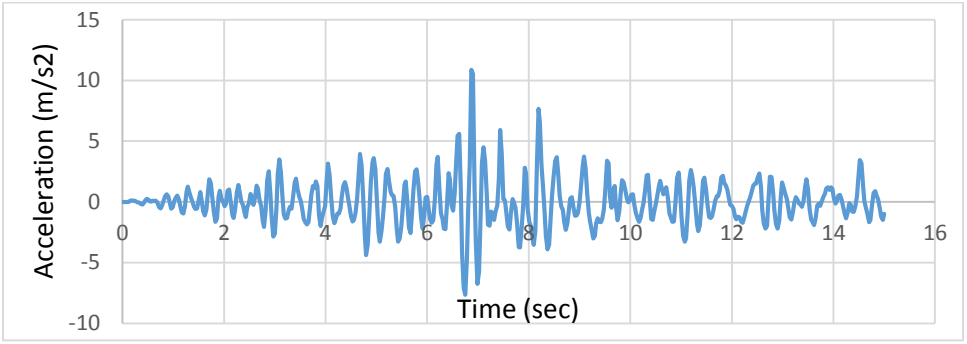

(b) Acceleration time history at crown (Max acceleration = 1.1g)

Displacement recorded at the base of structure

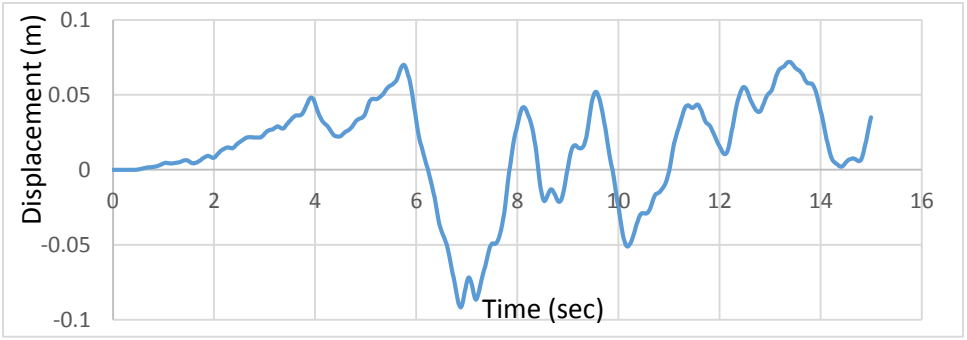

(c) Displacement time history at raft bottom

Displacement time history at the crown

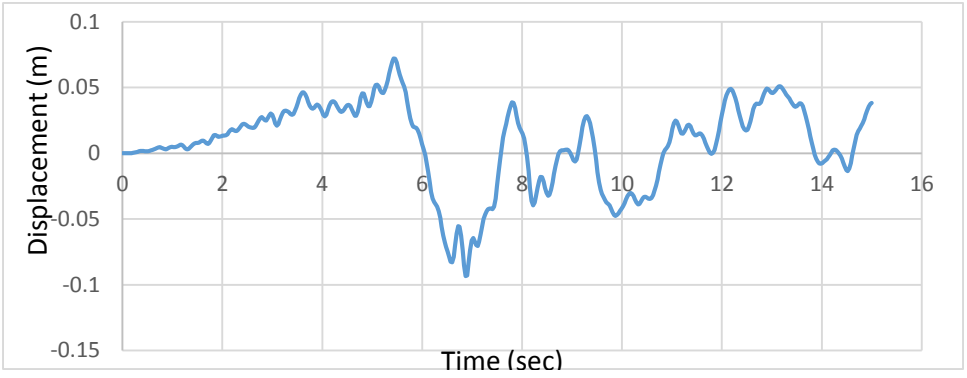

(d) Displacement time history at crown

Fig 4.28 Response recorded at the base of raft and crown of NPP for Northridge earthquake- Fixed base analysis

Maximum displacement of crown takes place at 5.42 sec, relative displacement of crown with respect to raft at 5.42 sec = (0.072 – 0.054) = 0.018m = 18mm

Case 2: Linear Soil Structure interaction

Earthquake motion shown in Fig. 4.22 is applied at base of soil model. This motion has maximum acceleration equal to 0.3g

Acceleration recorded at raft bottom

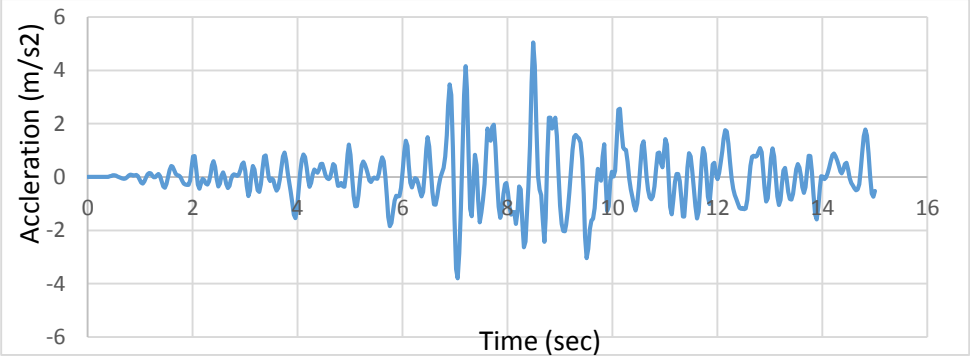

Max acceleration = 0.51 g

(a) Acceleration time history at bottom of raft

Acceleration recorded at the crown

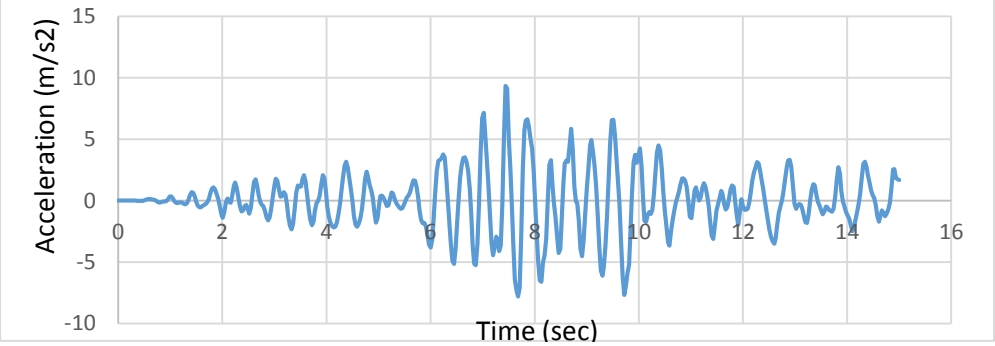

(b) Acceleration time history at crown (Max acceleration = 0.95 g)

Displacement recorded at Raft bottom

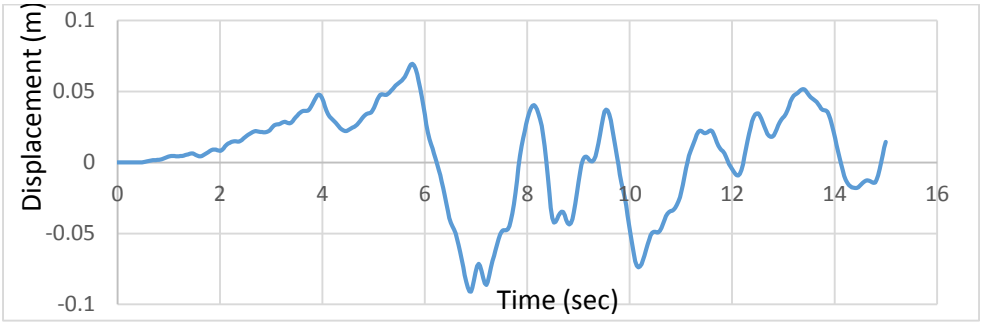

(c) Displacement time history at raft bottom

Displacement recorded at Crown

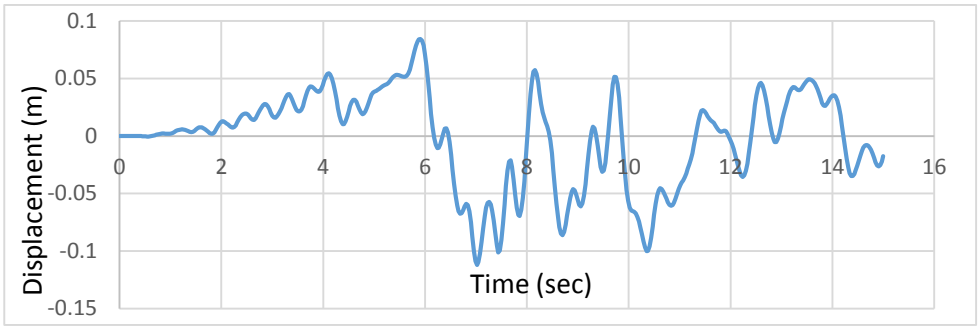

(d) Displacement time history at crown

Fig 4.29 Response recorded at the base of raft and crown of NPP for Northridge earthquake- Linear SSI

Maximum displacement of crown takes place at 7.02 sec, relative displacement of crown with respect to raft at 7.02 sec = (0.11224 – 0.07299) = 0.039m = 39mm

Case3: Nonlinear Soil-Structure interaction

Acceleration recorded at base of raft

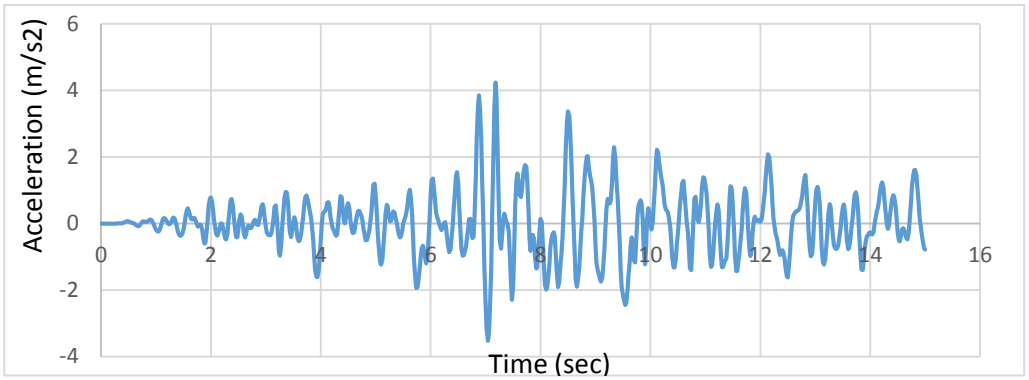

Max acceleration = 0.43 g

(a) Acceleration time history at bottom of raft

Acceleration recorded at Crown

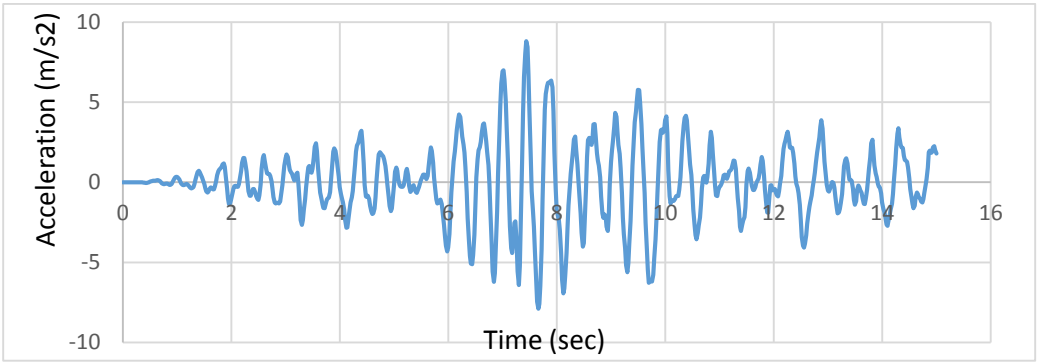

Max acceleration = 0.89 g

Fig 4.14 Acceleration time history at crown

Displacement recorded at the bottom of raft

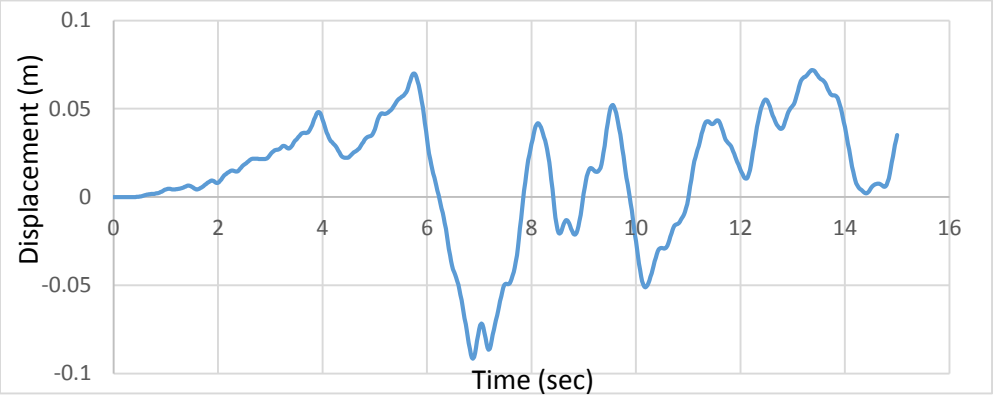

(c) Displacement time history at bottom of raft

Displacement time history at Crown

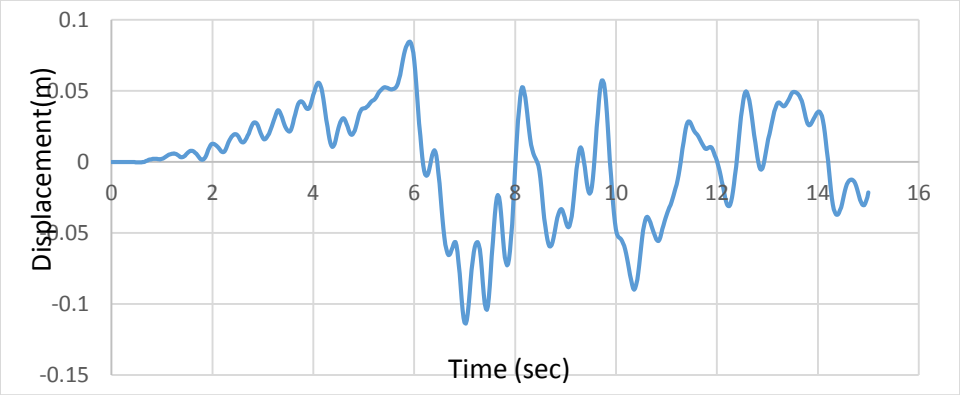

(d) Displacement time history at crown

Fig 4.30 Response recorded at the base of raft and crown of NPP for Northridge earthquake- Nonlinear SSI

Maximum displacement of crown takes place at 7.02 sec, relative displacement of crown with respect to raft at 7.02 sec = (0.1138 – 0.07262) = 0.041m = 41mm

Following table gives comparative study of response of NPP for all the three cases.

Table 4.2 Comparison of Response obtained for Fixed base, linear SSI and Nonlinear SSI of NPP

Type of Analysis	Acceleration at Crown (m/s^2)	Relative displacement of Crown w.r.t Raft(mm)
Fixed Base analysis	10.80	18
Linear SSI-Time history analysis	9.32	39
Nonlinear SSI-Time history analysis	8.73	41

4.6.2 Results of Loma-Prieta Time History Analysis

Case1: Fixed base analysis

Case 2: Linear soil-structure interaction analysis

Case3: Nonlinear soil-structure interaction analysis

Case 1: Fixed Base Time history Analysis of Structure

Acceleration time history at the base of raft

It is the time history obtained at the surface of soil after performing ground response analysis of rock outcrop motion considering nonlinear properties of soil.

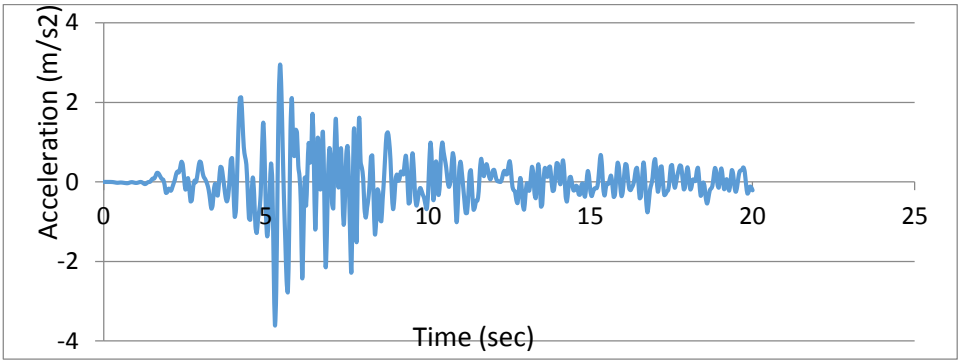

(a) Acceleration time history at raft bottom (Max acceleration = 0.36g)

Acceleration recorded at the crown

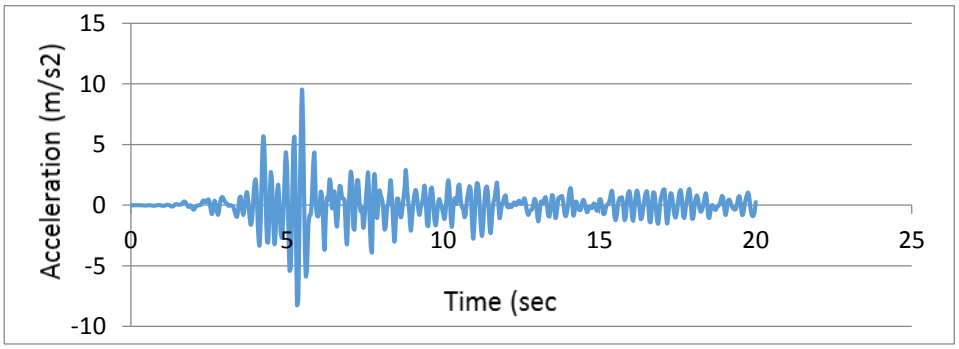

(b) Acceleration time history at crown (Max acceleration = 0.97g)

Displacement recorded at the base of structure

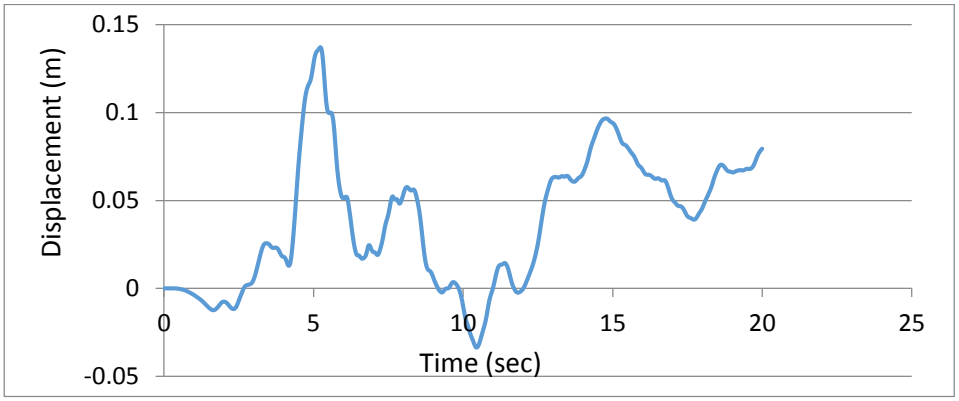

(c) Displacement time history at raft bottom

Displacement recorded at the crown

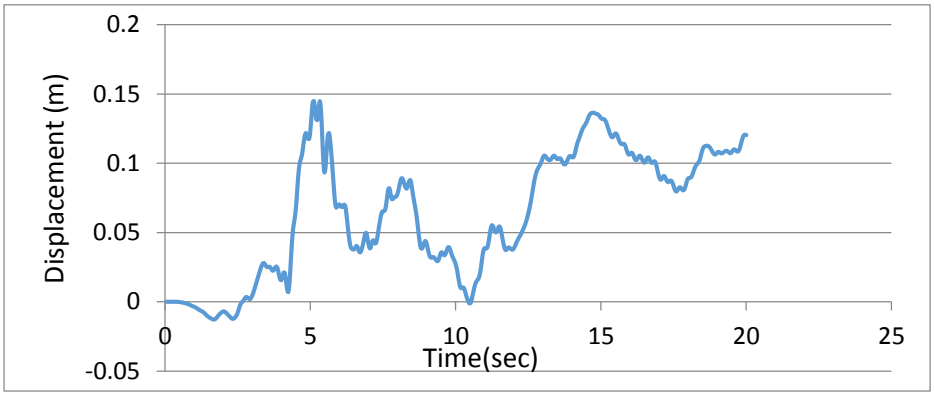

(d) Displacement time history at crown

Fig 4.31 Response recorded at the base of raft and crown of NPP for Loma-Prieta earthquake- Fixed Base Analysis

Maximum displacement of crown takes place at 10.44 sec, relative displacement of crown with respect to raft at 10.44 sec = (0.0001 – 0.0336) = 0.033m = 33mm

Case 2: Linear Soil Structure interaction

Earthquake motion shown in Fig. 4.24 is applied at base of soil model. This motion has maximum acceleration equal to 0.26g

Acceleration recorded at raft bottom

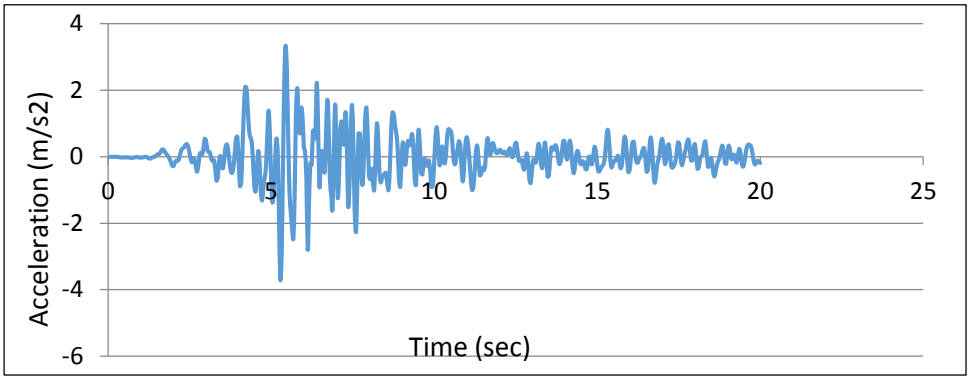

Max acceleration = 0.38 g

(a) Acceleration time history at bottom of raft

Acceleration recorded at the crown

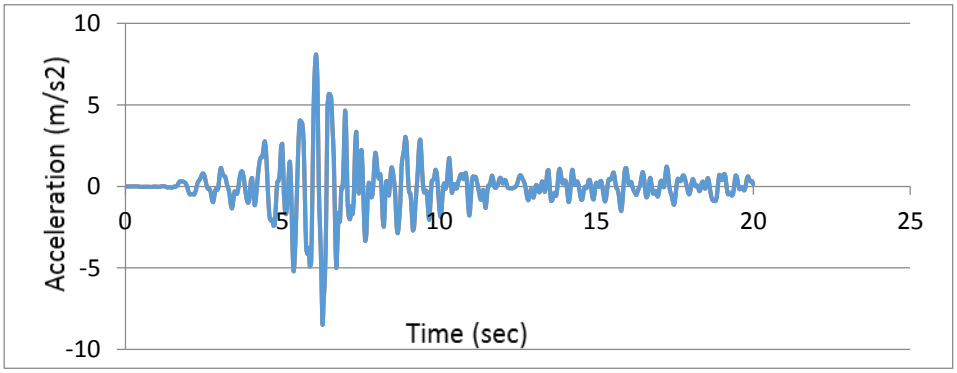

Max acceleration = 0.82 g

(b) Acceleration time history at crown

Displacement recorded at Raft bottom

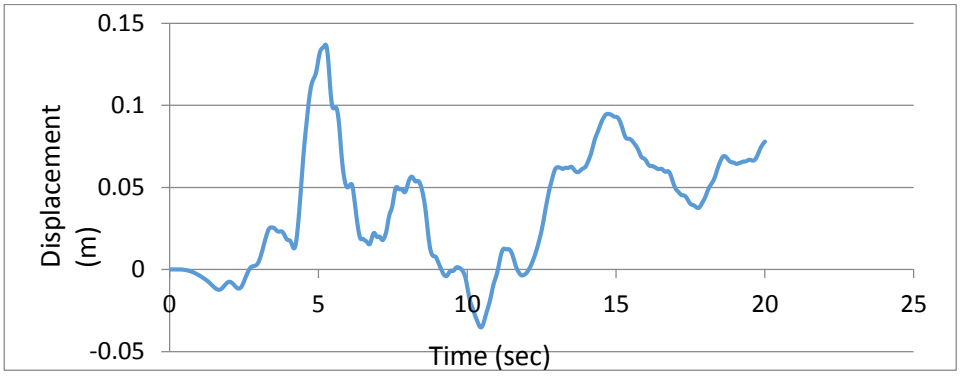

(c) Displacement time history at raft bottom

Displacement recorded at Crown

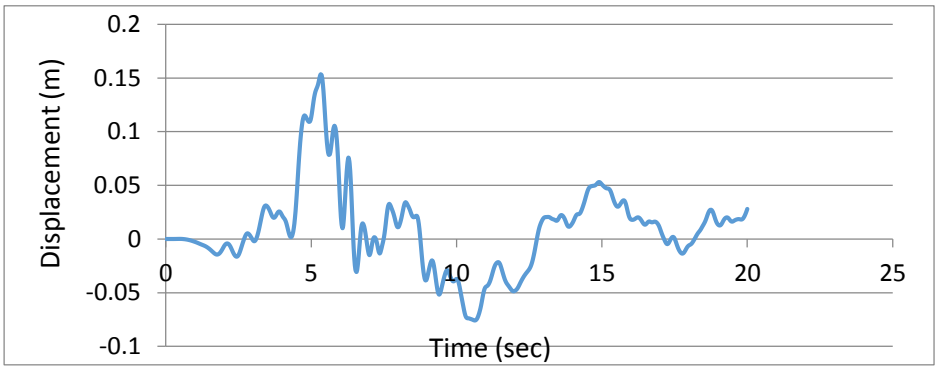

(d) Displacement time history at crown

Fig 4.32 Response recorded at the base of raft and crown of NPP for Loma-Prieta earthquake- Linear SSI

Maximum displacement of crown takes place at 10.64 sec, relative displacement of crown with respect to raft at 10.64 sec = (0.07584 – 0.0264) = 0.049m = 49mm

Case3: Nonlinear Soil-Structure interaction

Acceleration recorded at base of raft

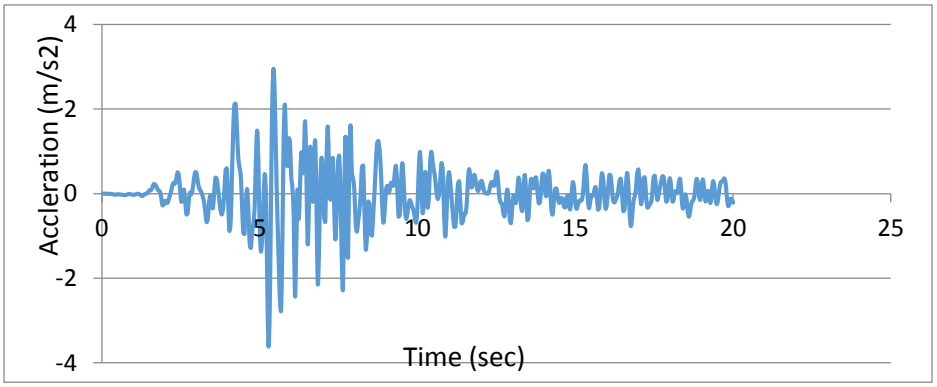

Max acceleration = 0.36 g

(a) Acceleration time history at bottom of raft

Acceleration time history at Crown

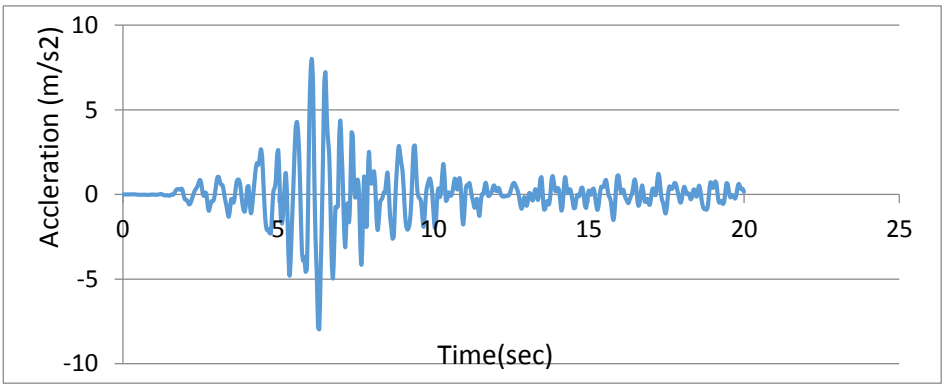

Max acceleration = 0.8 g

(b) Acceleration time history at crown

Displacement recorded at the bottom of raft

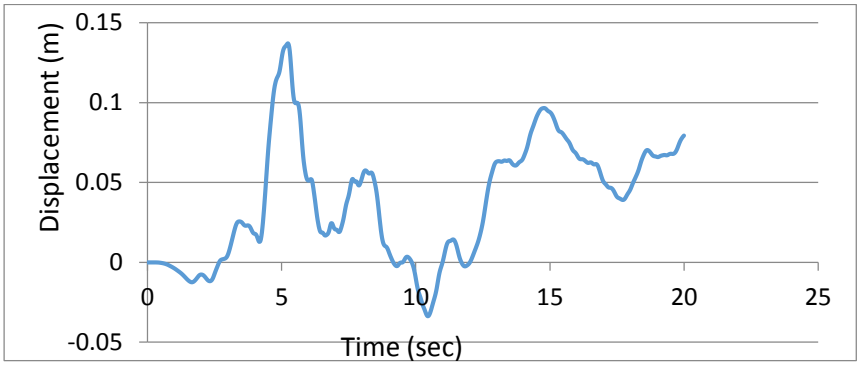

(c) Displacement time history at bottom of raft

Displacement recorded at Crown

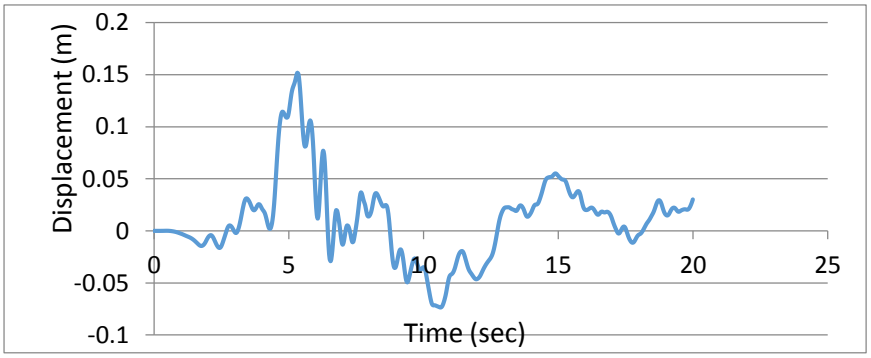

(d) Displacement time history at crown

Fig 4.33 Response recorded at the base of raft and crown of NPP for Loma-Prieta earthquake- Nonlinear SSI

Maximum displacement of crown takes place at 10.64 sec, relative displacement of crown with respect to raft at 10.64 sec = (0.07365 – 0.02554) = 0.048m = 48mm

Following table gives comparative study of response of NPP for all the three cases.

Table 4.3 Comparison of Response obtained for Fixed base, linear SSI and Nonlinear SSI of NPP

Type of Analysis	Acceleration at Crown (m/s^2)	Relative displacement of Crown w.r.t Raft(mm)
Fixed Base analysis	9.55	33
Linear SSI-Time history analysis	8.05	49
Nonlinear SSI-Time history analysis	7.80	48

4.6.3 Results of Kobe Time History Analysis

Case1: Fixed base analysis

Case2: Linear soil-structure interaction analysis

Case3: Nonlinear soil-structure interaction analysis

Case 1: Fixed Base Time history Analysis of Structure

Acceleration time history at the base of raft

It is the time history obtained at the surface of soil after performing ground response analysis of rock outcrop motion considering nonlinear properties of soil.

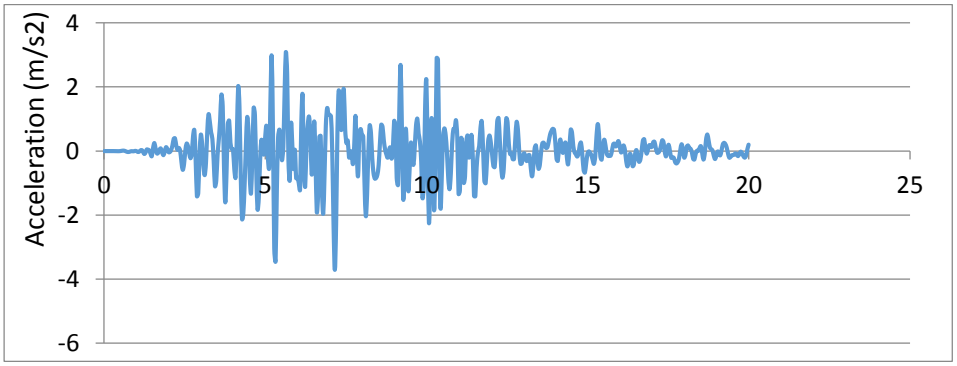

(a) Acceleration time history at raft bottom (Max acceleration = 0.37g)

Acceleration recorded at the crown

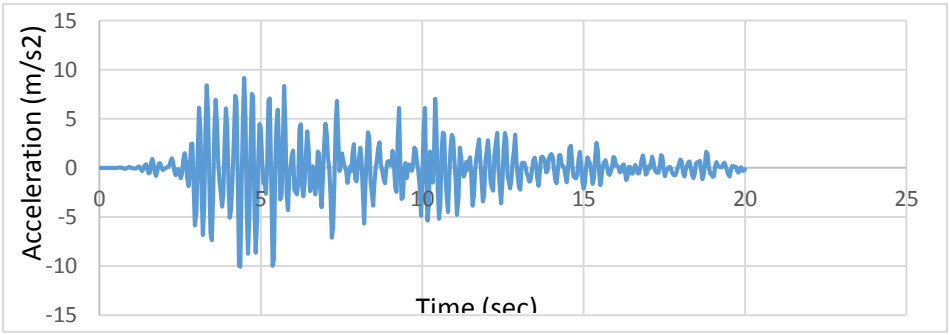

(b) Acceleration time history at crown (Max acceleration = 1.03g)

Displacement recorded at the base of structure

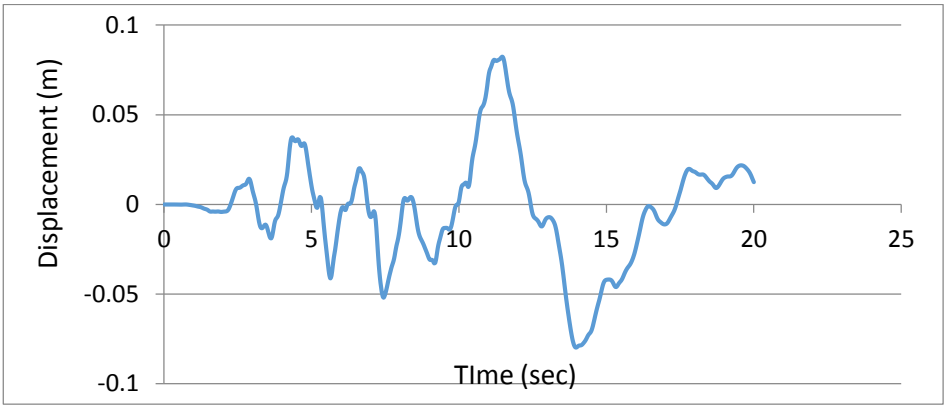

(c) Displacement time history at raft bottom

Displacement recorded at the crown

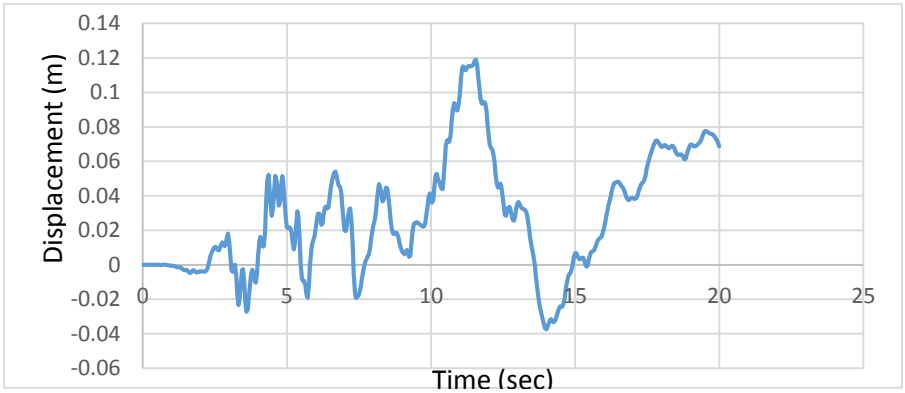

(d) Displacement time history at crown

Fig 4.34 Response recorded at the base of raft and crown of NPP for Kobe earthquake- Fixed base analysis

Maximum displacement of crown takes place at 11.56 sec, relative displacement of crown with respect to raft at 11.56 sec = (0.118 – 0.077) = 0.041m = 41mm

Case 2: Linear Soil Structure interaction

Earthquake motion shown in Fig. 4.26 is applied at base of soil model. This motion has maximum acceleration equal to 0.27g

Acceleration recorded at raft bottom

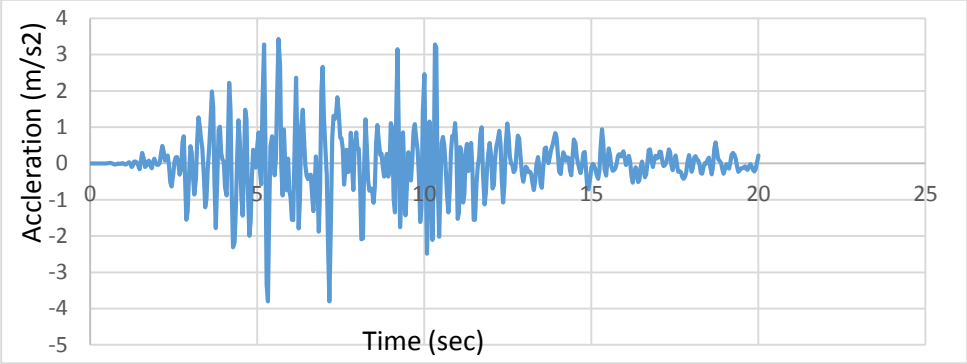

Max acceleration = 0.39 g

(a) Acceleration time history at bottom of raft

Acceleration recorded at the crown

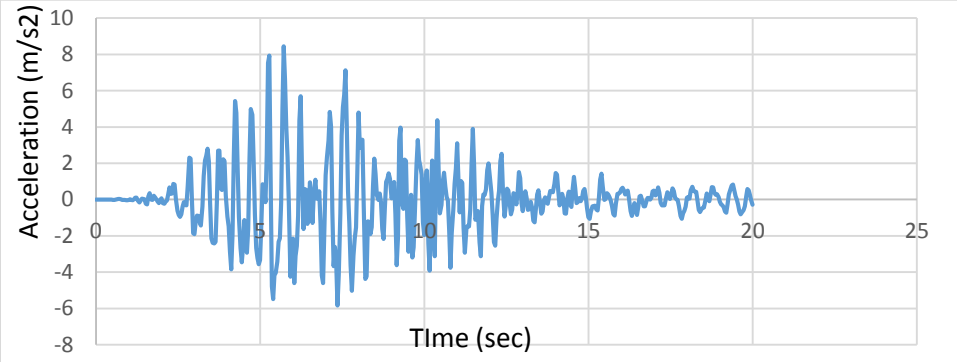

Max acceleration = 0.86 g

(b)Acceleration time history at crown

Displacement recorded at Raft bottom

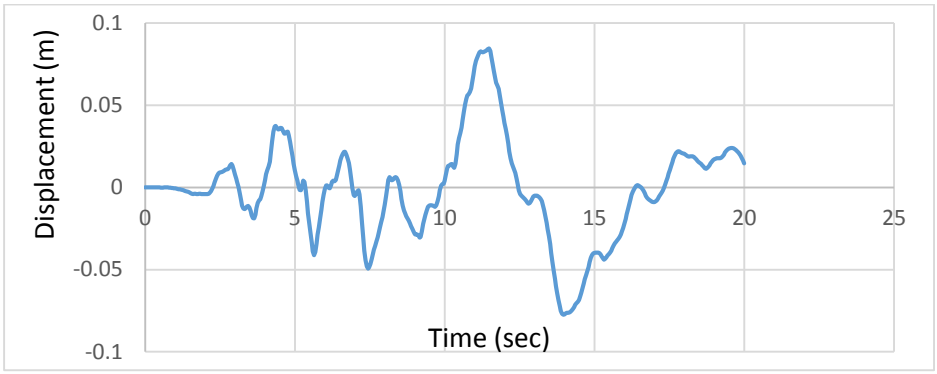

(c) Displacement time history at raft bottom

Displacement recorded at Crown

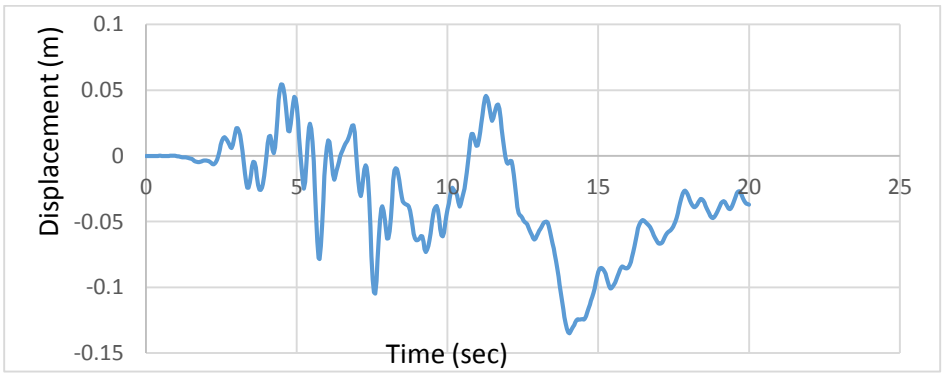

(d) Displacement time history at crown

Fig 4.35 Response recorded at the base of raft and crown of NPP for Kobe earthquake-Linear SSI

Maximum displacement of crown takes place at 14.04 sec, relative displacement of crown with respect to raft at 14.04 sec = (0.135 – 0.076) = 0.058m = 58mm

Case2: Nonlinear Soil-Structure interaction

Acceleration recorded at base of raft

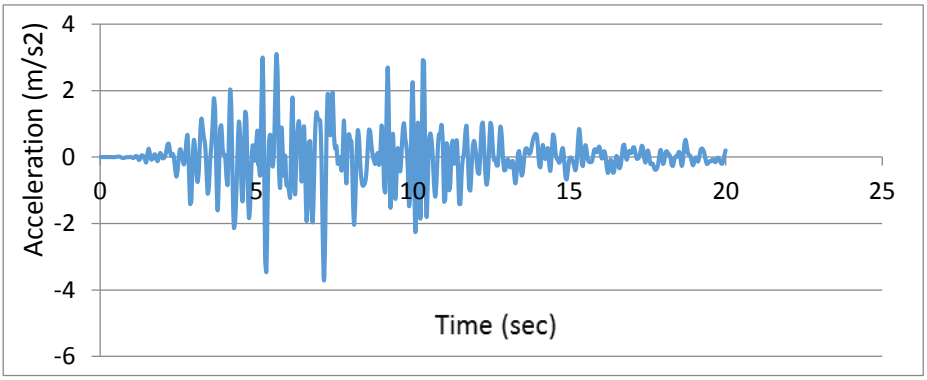

Max acceleration = 0.37 g

(a) Acceleration time history at bottom of raft

Acceleration recorded at Crown

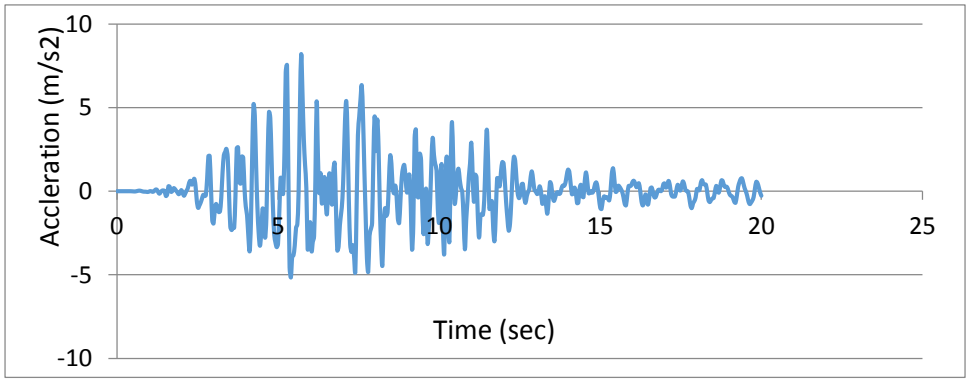

Max acceleration = 0.82 g

(b) Acceleration time history at crown

Displacement recorded at the bottom of raft

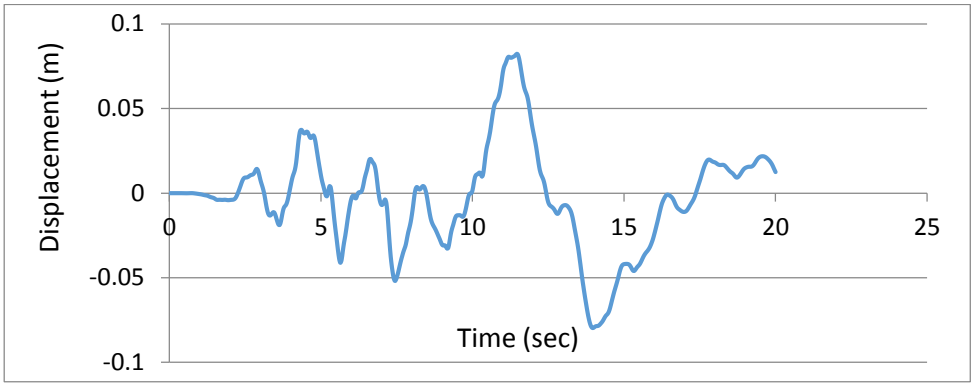

(c) Displacement time history at bottom of raft

Displacement recorded at Crown

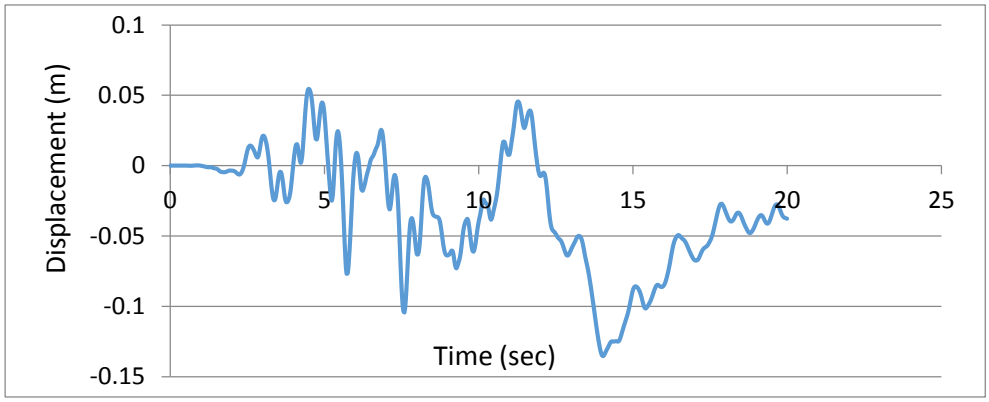

(d) Displacement time history at crown

Fig 4.36 Response recorded at the base of raft and crown of NPP for Kobe earthquake-Nonlinear SSI

Maximum displacement of crown takes place at 14.04 sec, relative displacement of crown with respect to raft at 14.04 sec = (0.135 – 0.079) = 0.056m = 56mm

Following table gives comparative study of response of NPP for all the three cases.

Table 4.4 Comparison of Response obtained for Fixed base, linear SSI and Nonlinear SSI of NPP for Kobe Earthquake

Type of Analysis	Acceleration at Crown (m/s^2)	Relative displacement of Crown w.r.t Raft(mm)
Fixed Base analysis	10.08	41
Linear SSI-Time history analysis	8.45	58
Nonlinear SSI-Time history analysis	8.22	56

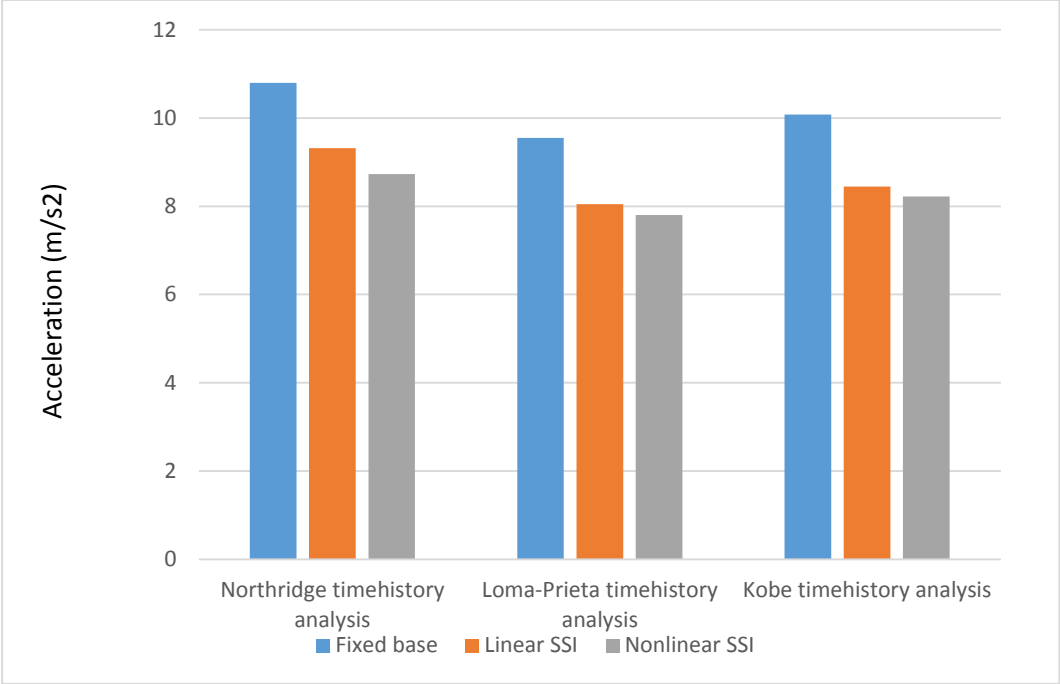

(a)

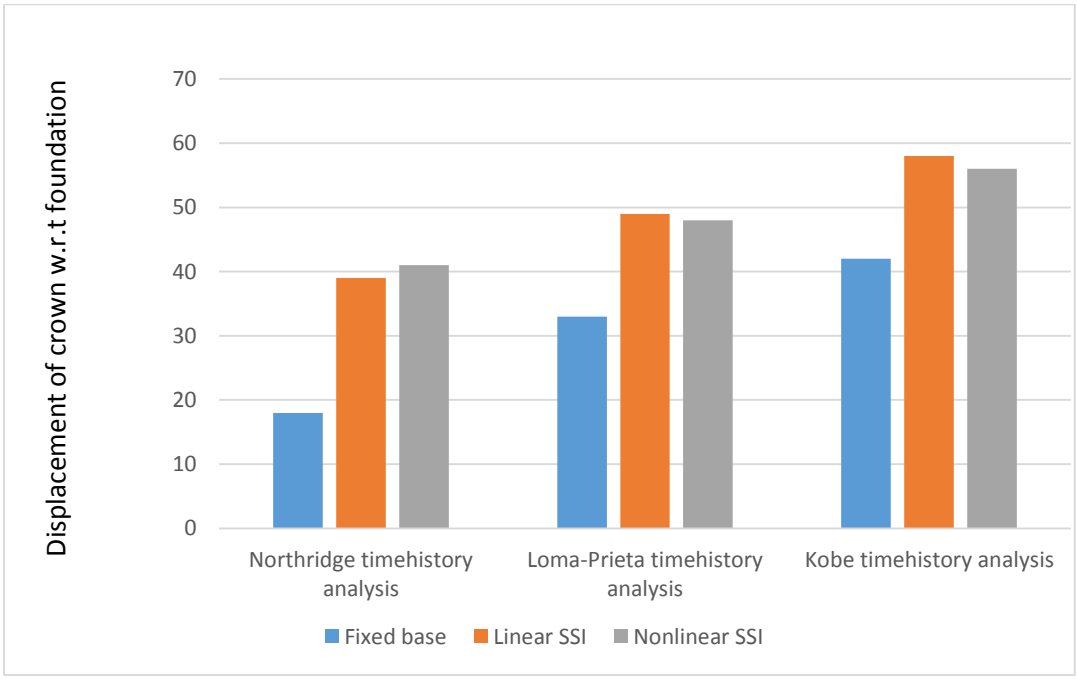

(b)

Fig 4.37 Effect of soil structure interaction on response of structure

4.6.4 Results of Northridge-Three Components Earthquake analysis

The deconvoluted motion of northridge earthquake shown in Fig4.22 is applied in both the horizontal direction. 2/3rd of this component is applied in vertical direction.

Results of **nonlinear soil-structure interaction** has been shown in following figures.

X and Z-directions are two horizontal orthogonal directions whereas Y- direction shows vertical direction. Only X-direction results are shown below for comparison with previously shown 1 component earthquake analysis.

X-Direction

Earthquake motion shown in Fig. 4.22 is applied at base of soil model. This motion has maximum acceleration equal to 0.29g

Acceleration time history at the base of raft

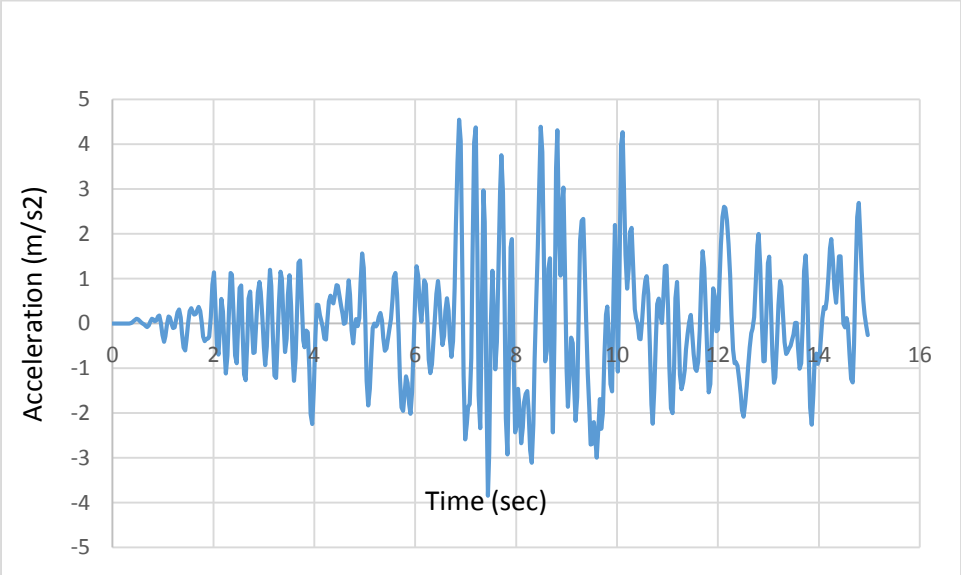

(a) Acceleration time history at raft bottom (Max acceleration = 0.46g)

Acceleration recorded at the crown

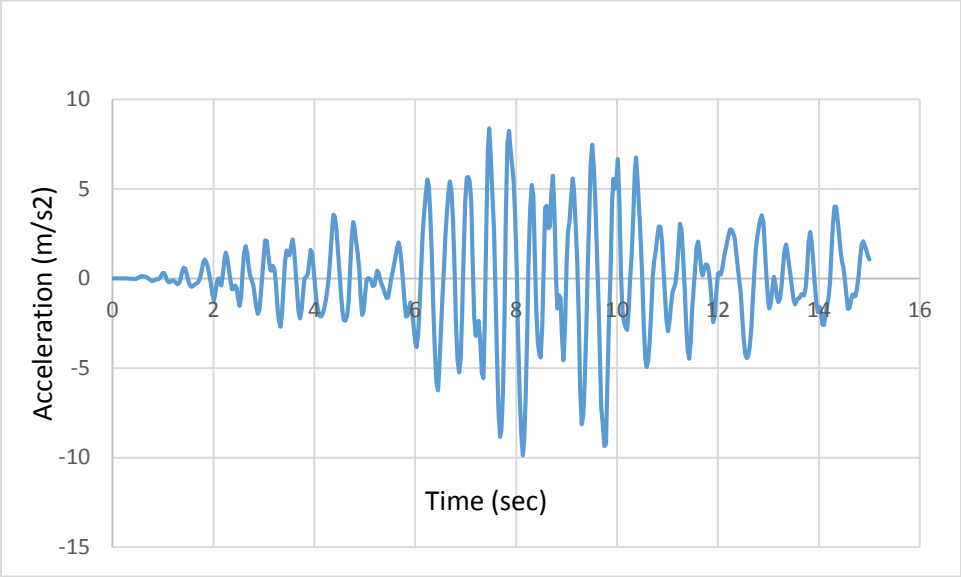

(b) Acceleration time history at crown (Max acceleration = 0.98g)

Displacement recorded at the base of structure

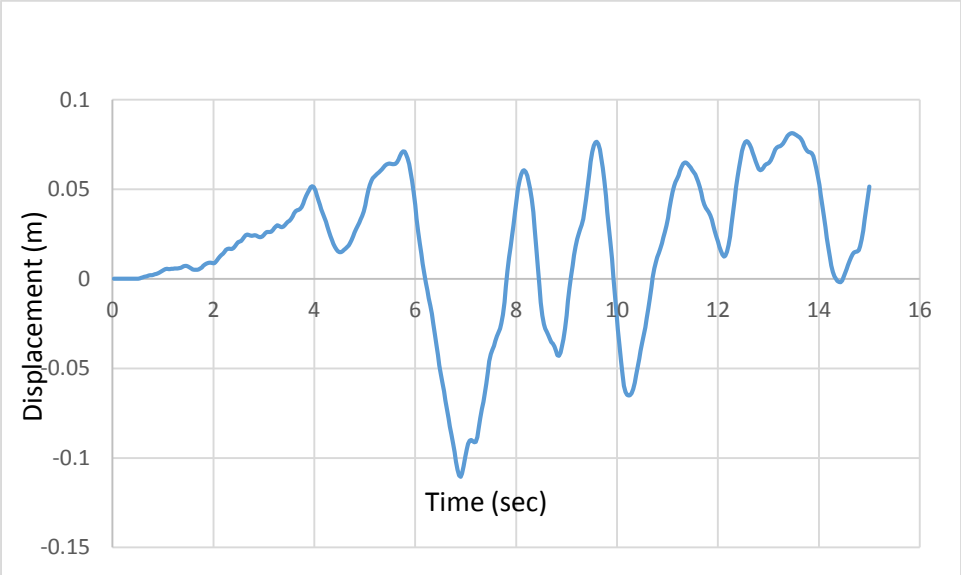

(c) Displacement time history at raft bottom

Displacement recorded at the crown

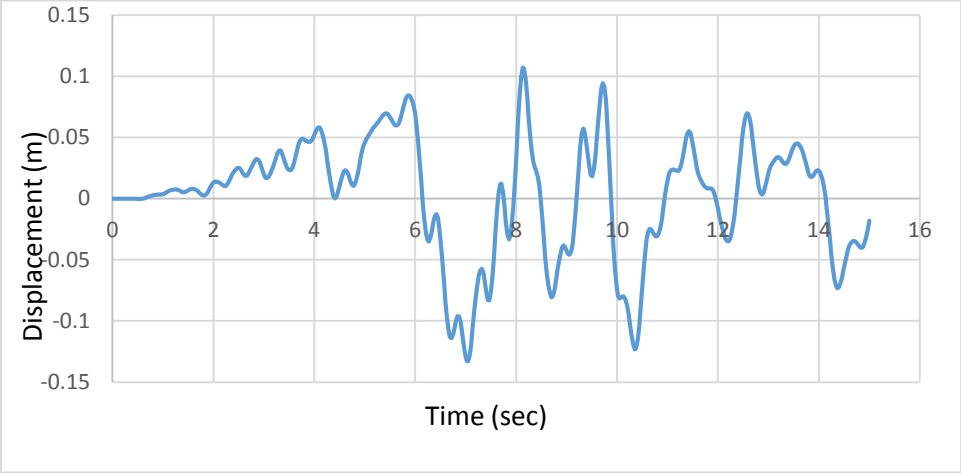

(d) Displacement time history at crown

Fig 4.38 Response recorded at the base of raft and crown of NPP for Northridge 3C earthquake- Nonlinear SSI

Maximum displacement of crown takes place at 8.13 sec, relative displacement of crown with respect to raft at 8.13 sec = (0.107 – 0.060) = 0.047m = 47mm

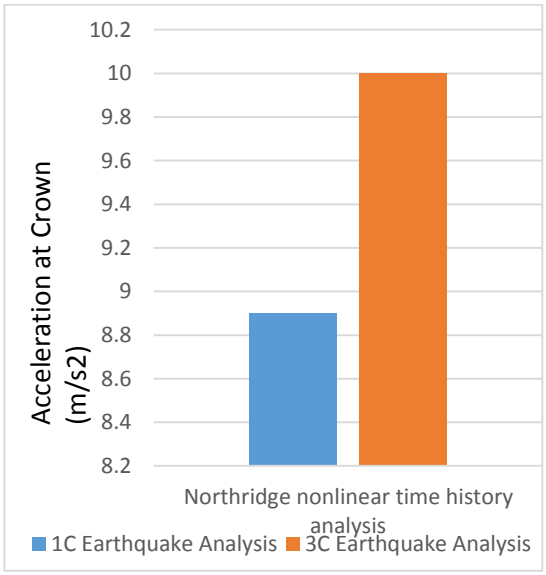

(a)

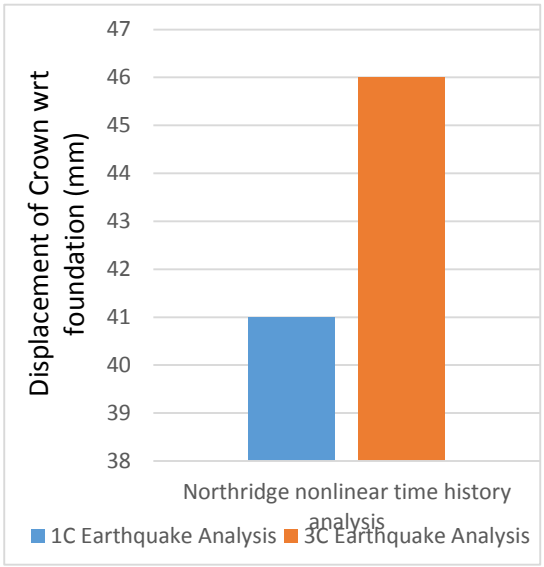

(b)

Fig 4.39 Comparison of response obtained in X-direction for 1C and 3C earthquake excitation with nonlinear Soil structure interaction

The above comparison between one component and three component earthquake excitations, shows that, 3D loading leads to multiaxial stress interaction. This interaction reduces soil strength and increases nonlinearity of soil. The shear modulus of soil decreases and dissipation of energy increases.

4.7 Damage Study of Superstructure

The NPP structure is studied for damage occurred during different intensities of earthquake. Following figures show extent of damage in structure considering nonlinear soil structure interaction. Fig.4.40 (a) shows the damage when deconvoluted Northridge is applied at the base of soil having maximum acceleration 0.29g. Next, in Fig.4.40(b) the damage is shown for 1.25 times deconvoluted Northridge acceleration time history(0.36g). Fig.4.40 (c) shows the damage for 1.5 times the deconvoluted Northridge acceleration time history (0.435g).

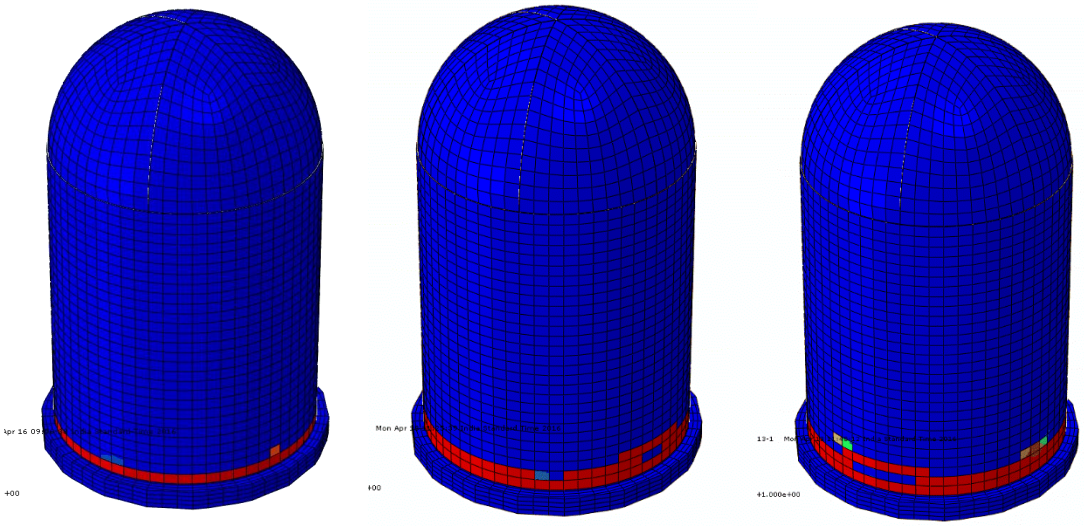

(a) (b) (c)

Fig.4.40 Comparison of Tension Damage for increasing acceleration of earthquake

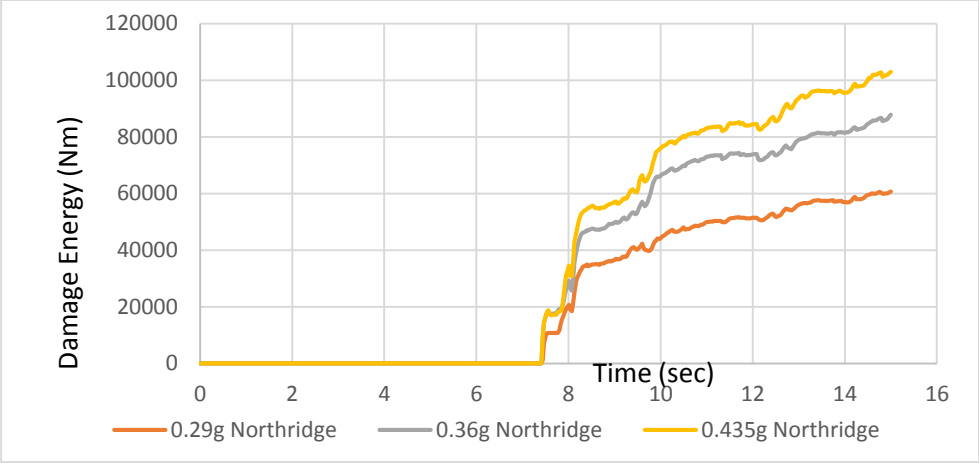

Fig.4.41 Damage energy in cylinder with increasing acceleration

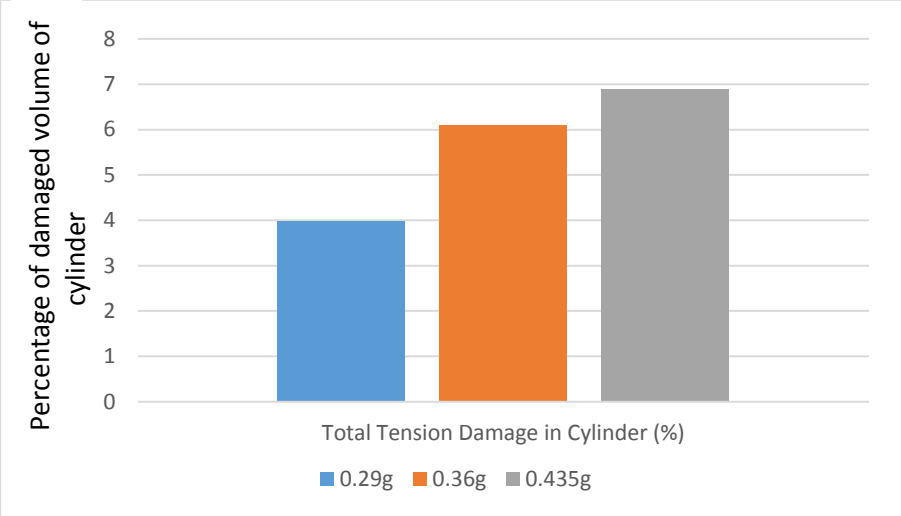

Fig.4.42 Percentage of volume damaged in cylinder with increasing acceleration

Above figures show that, with increase in intensity of earthquake, total damage in cylinder also increased. Damage starts from the base and propagates towards dome of structure.

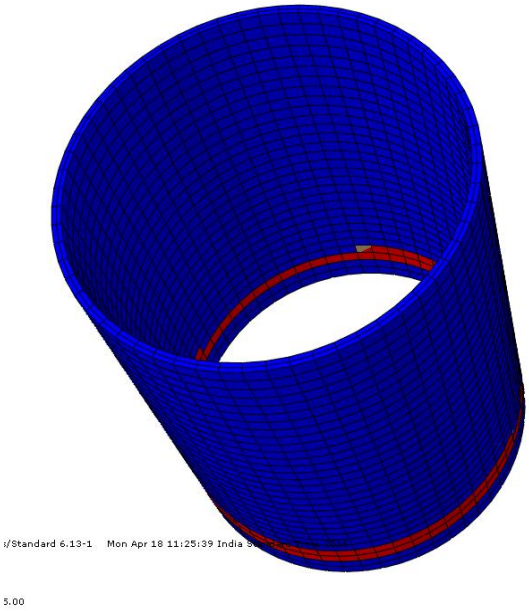

This figure shows tension damage on inner and outer face of cylinder for 0.36g Northridge applied at the base soil considering nonlinear SSI. Figure shows that tension damage is more on outer face of cylinder as compare to inner face.

Fig.4.43 Tension damage on inner and outer face

Damage comparison of fixed base structure with structure considering nonlinear SSI

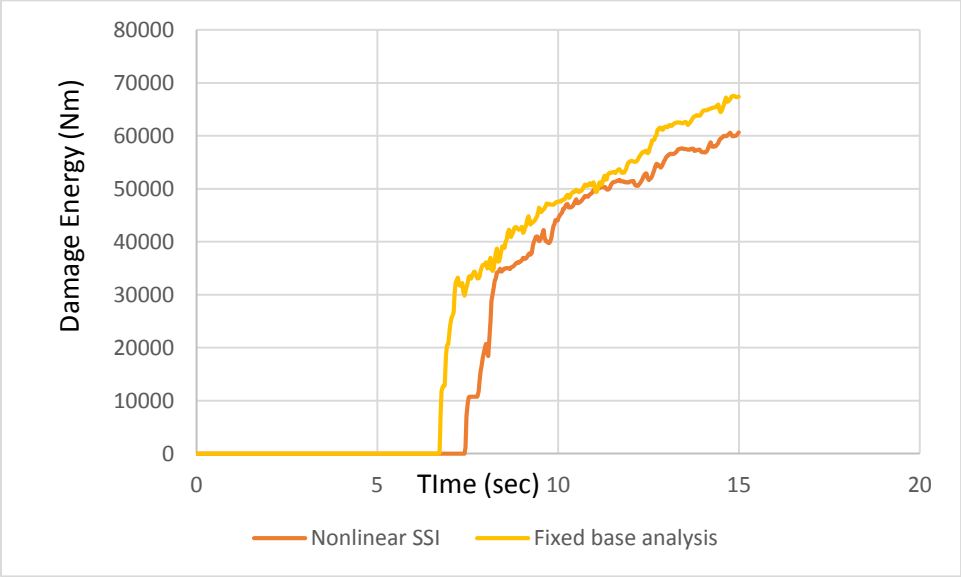

Fig.4.44 Comparison of damage for fixed base and nonlinear SSI analysis

(This study is for Northridge time history. Refer section 4.6.1 for details)

Above Fig.4.44 shows that nonlinear SSI gives less damage as compare to fixed base analysis. Nonlinear SSI gives more realistic result, and less damage results in economical design of structure.

Effect of reinforcement on damage

Following Fig 4.45 shows that tension damage occurred in the wall of containment structure without reinforcement is more than tension damage occurred when reinforcement is provided in containment structure. Thus, reinforcement controls the progress of damage in the structure.

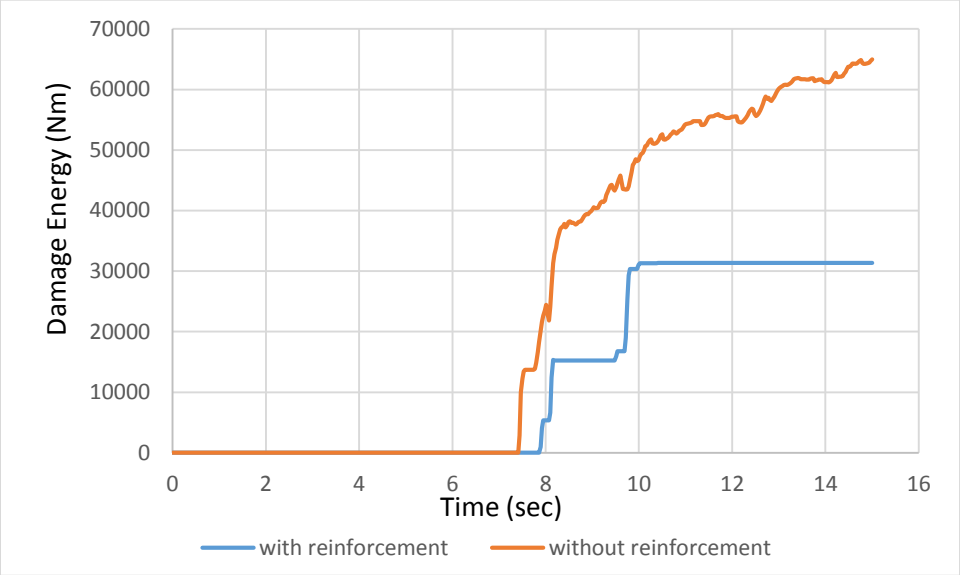

Fig.4.45 Effect of reinforcement on tension damage

5. CONCLUSIONS

The seismic response of containment structure of NPP has been investigated numerically. The 3D numerical modelling of containment structure and the surrounding soil has been developed. The reinforcement in the containment structure has also been modelled. The nonlinearity in the concrete is modelled by concrete damage plasticity model, the nonlinearity of soil is modelled by mohr-coulomb yield criteria and the nonlinearity in reinforcement is modelled by nonlinear stress strain relation. The soil-structure interaction considering the finite energy absorbing soil boundaries is considered. Following are the observations from the study.

1. Introduction of soil beneath the structure elongated the period of structure from 0.24sec to 0.44 sec for the soil type considered, indicating increased flexibility of the overall structure.

2. Following table shows comparison of acceleration measured at the crown of NPP containment structure. The comparison shows that accelerations obtained in case of fixed base analysis are greater than that of obtained from soil structure interaction analysis. Linear SSI analysis gives more acceleration as compare to nonlinear SSI. Thus, nonlinear SSI shows reduction in accelerations as a result of dissipation of energy due to nonlinearity.

	Acceleration at crown (m/s^2)		
Time history	Fixed base analysis	Linear SSI	Nonlinear SSI
Northridge	10.80	9.32	8.73
Loma-Prieta	9.55	8.02	7.80
Kobe	10.08	8.45	8.22

3. Following table gives the comparison of displacement measured at crown of containment structure. The displacements obtained for fixed base are lesser than displacement obtained with soil structure interaction.

Time history	Displacement of crown (mm)		
	Fixed base analysis	Linear SSI	Nonlinear SSI
Northridge	18	39	41
Loma-Prieta	33	49	48
Kobe	41	58	56

4. Three component Northridge earthquake excitation analysis when compared with one component Northridge earthquake excitation analysis, showed that the crown acceleration measured in X-direction decreased from 9.61 m/s^2 to 8.73$m/s^{2.}$ Displacement of crown with respect to raft obtained in three component analysis is 47 mm which is greater than 41 mm obtained from one component analysis. This is because, 3D loading leads to multiaxial stress interaction. This interaction reduces soil strength and increases nonlinearity of soil. The shear modulus of soil decreases and dissipation of energy increases.

5. The study of containment damage under earthquake excitation shows that tension cracks are predominant in lower portion of the containment wall. No damage is observed in the raft. So crack checks need to be made for the walls.

6. The 3.97% damage of total volume of containment structure occurred when acceleration time history with PGA 0.29g was applied at the base of the soil. This percentage increased to 6.1 % and 6.9% when acceleration time histories with PGA values 0.36g and 0.435g were applied at the base of soil respectively. This tension damage was observed initially at the lower portion of wall which grew towards the upper part of containment structure with increase in intensity of earthquake excitation.

7. Tension cracks are dominant on outer face of the containment wall as compared to the inner face wall.

8. Fixed base analysis gives unrealistically more tension damage as compare to the damage obtained considering nonlinear SSI. In present study, nonlinear SSI analysis has reduced tension damage by 11% as compare to damage obtained from fixed base analysis.

9. In present study of damage, presence of reinforcement has reduced tension damage in the containment structure by 52%. Thus, provision of reinforcement in the structure controls the amount of tension damage for the earthquake considered.

REFERENCES

[1] Nptel, “http://nptel.ac.in/courses/105101004/6.” .

[2] Agarwal.P and Shrikhande.M, *Earthquake Resistant Design of Structures*. Prentice Hall of India, New Delhi., 2013.

[3] Kumar.S, Raychowdhury.P, and Gundlapalli.P, “Response analysis of a nuclear containment structure with nonlinear soil – structure interaction under bi-directional ground motion,” *Int. J. Adv. Struct. Eng.*, pp. 211–221, 2015.

[4] Cheng Y M, “The Use of Infinite Element,” *Comput. Geotech.*, vol. 18, no. 1, pp. 65–70, 1996.

[5] Venancio-filho.F, Barros.F.C.P.De, Almeida.M.C.F, and Ferreira.W.G, “Soil-structure interaction analysis of NPP containments : substructure and frequency domain methods,” vol. 174, pp. 165–176, 1997.

[6] Ghiocel.D.M, “Seismic motion incoherency effects on soil-structure interaction response of nuclear power plant buildings,” *Proceedings, 10th Int. Conf. Struct. Saf. Reliab. Osaka, Japan.*, 2009.

[7] Kawasato.T, Okutani.T, Ishikawa.T, Fujimori.T, and Akimoto.M, “Experimental Study of Seismic Soil-Structure Interaction by using Large Geotechnical Centrifuge System,” *14th World Conf. Earthq. Eng.*, 2008.

[8] Raychowdhury.P and Hutchinson.T. C, “Performance evaluation of a nonlinear Winkler-based shallow foundation model using centrifuge test results,” *Earthq. Eng. Struct. Dyn.*, vol. 38, no. March, pp. 679–698, 2009.

[9] Saxena.N, Paul.D.K, and Kumar.R, “Effects of slip and separation on seismic SSI response of nuclear reactor building,” *Nucl. Eng. Des.*, vol. 241, no. 1, pp. 12–17, 2011.

[10] Lopamudra.B and Raychowdhury.P, “Seismic response analysis of a nuclear reactor structure considering nonlinear soil-structure interaction,” *Nucl. Eng. Des.*, vol. 265, pp. 1078–1090, 2013.

[11] Saxena.N and Paul.D.K, “Effects of embedment including slip and separation on seismic SSI response of a nuclear reactor building,” *Nucl. Eng. Des.*, vol. 247, pp. 23–33, 2012.

[12] Samangany.A.Y, Naderi.R, Hosein.M, and Hadi.T, “Static and Dynamic Analysis of Storage Tanks Considering Soil-Structure Interaction,” *Int. Res. J. Appl. Basic Sci.*, vol. 6, no. 4, pp. 515–532, 2013.

[13] Kumar.V and Maheshwari.B .K, “Fe modelling of npp for dynamic loads considering ssi,” *Proc. Indian Geotech. Conf. Roorkee*, 2013.

[14] Shionozuka.M, Hawang.H, and Reich.M, “Reliability assesment of reinforced concrete containment structures,” *Nucl. Eng. Des.*, vol. 80, no. 14, pp. 247–267, 1984.

[15] *Analysis Users Guide Manual,Abaqus 6.13*, vol. III. .

[16] Nptel, “http://nptel.ac.in/courses/105103097/web/chap9final/s2.htm.” .

[17] Jankowiak.T and Lodygowskl.T, “Identification of parameters of concrete damage plasticity constitutive model,” *Found. Civ. Environ. Eng.*, vol. 6, 2005.

[18] Properties of Soils APPC, “http://www.academia.edu/8149496/APPC-Soil_Properties.” .

[19] Marzban.S, Banazadeh.M, and Azarbakht.A, “Seismic performance of reinforced concrete shear wall frames considering soil– foundation–structure interaction.,” *Proc. 8th Int. Conf. Struct. Dyn. Leuven*, 2011.

[20] Kramer, *Geotechnical Earthquake Engineering*. 1996.

[21] Hashash.Y.M.A, “Deepsoil User Manual Version 6.1,” 2015.